Advanced Dynamic spectrum
5G mobile networks Employing
Licensed shared access

Advanced Dynamic spectrum 5G mobile networks Employing Licensed shared access

Grant Agreement for: Collaborative project
Project acronym: ADEL
Grant Agreement number: 619647

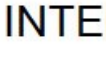

Advanced Dynamic spectrum 5G mobile networks Employing Licensed shared access

This project has received funding from the European Union's Seventh Framework Programme for research, technological development and demonstration under grant agreement no. 619647.

Project Deliverable D5.3:

Cooperative Communication Techniques for LSA

Contractual Date of Delivery:	1 June 2016
Actual Date of Delivery:	30 July 2016
Editors:	Tharmalingam Ratnarajah, Faheem Khan
Authors:	Tharmalingam Ratnarajah, Faheem Khan, Miltiadis Filippou, Sudip Biswas, Y He, Constantinos Papadias, Konstantinos Ntougias, Kostas Voulgaris, George Papageorgiou, Marius Pesavento, Kalyana Gopala, Dirk Slock, Nicola Marchetti, Marius Pesavento
Work package title:	WP5 – Dynamic spectrum access
Work package leader:	UEDIN
Contributing partners:	AIT, TUDA, EUR, TCD, PTIN, IMC
Nature	O[1]
Dissemination level	CO[2]
Version	1.3
Total Number of Pages:	50
File:	D5.3_Cooperative communication techniques for LSA_Final.pdf

[1] Nature of the Deliverable:
R = Report, P = Prototype, D = Demonstrator, O = Other

[2] Dissemination level codes:
PU = Public
PP = Restricted to other programme participants (including Commission Services)
RE = Restricted to a group specified by the consortium (including the Commission Services)
CO = Confidential, only for the members of the consortium (including the Commission Services)

Abstract: This deliverable presents a number of algorithms and schemes that facilitate cooperative communication between entities belonging to a LSA network with reference to the investigated scenarios and use cases.

Keywords: Licensed Shared Access (LSA), cooperation, coordination, cost efficiency, spectral efficiency, Cloud-Radio Access Network (C-RAN), Quality-of-Service (QoS), transmission design

Document Revision history

Version	Date	Send to	Summary of main changes	Approved by
V1.0	14-Dec-2015	ALL	Interim Draft – M24	T Ratnarajah
V1.1	15-May-2016	ALL	First Draft	T Ratnarajah
V1.2	15-June-2016	ALL	Second draft	T Ratnarajah
V1.3	30-July-2016	ALL	Final draft	T Ratnarajah

Executive Summary

This is the deliverable *D5.3 Cooperative Communication Techniques for LSA*, FP7 project ADEL (ICT- 619647). This work was carried out as part of WP5: Dynamic Spectrum Access. This deliverable relies on the work defined within task T5.3 detailed in the Description of Work.

In this deliverable, a number of algorithms and schemes that facilitate cooperative communication between entities belonging to a LSA network, are described, with reference to the investigated scenarios and use cases. A brief summary of deliverable is given below:

- Focusing on the small-cell/cloud-Radio Access Network (C-RAN) scenario, the case where a number of users requires a wireless service from a Virtual Mobile Network Operator (VMNO), is studied. Motivated by the above situation, a cost efficiency metric is proposed, and then, based on that, as well as on the Zero-Forcing (ZF) distributed Multiple-Input-Multiple-Output (MIMO) precoding technique, the optimal solution is evaluated in terms of cost efficiency, in comparison to an arbitrary, uncoordinated strategy.
- The operation of a Multiple-Input-Single-Output (MISO) macro-cell LSA system in the downlink is investigated. The system is composed of an incumbent Mobile Network Operator (MNO), which coexists with a licensee MNO, in the lack of any spectrum sensing procedure carried out at the latter. Inspired by the underlay Cognitive Radio (CR) approach, a coordinated transmission scheme is designed, aiming at maximizing the average rate of the licensee, subject to an average rate constraint for the incumbent. A novel set of applicable precoding schemes is proposed, based on Matched Filter (MF) and statistical ZF (sZF) solutions.
- A macro-cell LSA scenario is considered in the downlink. Influenced by both underlay (i.e., spectrum sharing) and interweave (i.e., opportunistic) CR systems, the throughput performance of a hybrid interweave/underlay MIMO LSA system is examined. Exploiting the derived expressions, a new optimization problem is set up with respect to the SS parameters and then effectively solved, according to which the average rate of the licensee is maximized for a given outage constraint, imposed by the incumbent MNO.
- The uplink a macro-cell, hybrid LSA system is considered and the problem of jointly designing the SS parameters and the receive beamforming (BF) scheme, is tackled, in the presence of combined instantaneous and statistical CSIT, where the involved channels undergo correlated Rayleigh fading.
- The utilization of Opportunistic Beam-Forming (OBF) combined with Proportional Fair Scheduling (PFS) in the licensee network is considered in an LSA setup employing cooperation between the licensee and the incumbent. In the first considered use-case, a setup comprises of two macro-cells, one belonging to the incumbent and the other belonging to the licensee, with an overlapping sector. In the second use-case, a setup comprises of a macro-cell belonging to the incumbent and three partially overlapping small-cells within a sector of that macro-cell belonging to the licensee.
- The train scenario is considered in which the high mobility leads to Intercarrier Interference (ICI) in OFDM communication systems. However, even at TGV speeds, it turns out that in a

typical LTE setting, the channel time variation over an OFDM symbol duration can be adequately modelled by a linear variation. MIMO transmission techniques are then developed in which the excess multiple antennas over the spatial multiplexing are exploited to adequately suppress the ICI.

- LSA coordinated beamforming is considered between incumbent and licensee cells. Optimized beamforming techniques are introduced to maximize a joint weighted sum utility function. These techniques are furthermore extended to the case of partial CSIT, with a practical approximation of the ergodic sum utility function, which becomes exact in the Massive MIMO setting.
- Full-duplex spectrum sensing system is developed to realize the simultaneous spectrum sensing and secondary transmission. Firstly, the generalized expressions of the key sensing performance metrics are derived for multiple sensing antennas. Listen-and-talk protocol is applied and multiple sensing/transmission antennas are considered in this part. Secondly, the optimal decision threshold pair is investigated in order to minimize the total error rate of the system. Therefore, the benefits of primary and secondary users can be considered at the same time.
- The problem of effective spectrum sharing between a collocated Multiple-Input-Multiple-Output (MIMO) radar that monitors the existence of a target and a wireless communications system is considered. An accurate model is presented for the operation of the wireless system in the downlink, while the MIMO radar tries to maintain an acceptable detectability level of a target in the far field. The target detection problem is reformulated using a sensing approach based on energy detection, while the BS applies beamforming to null the interference created at the radar receiver.
- A full-duplex (FD) multiple-input multiple-output (MIMO) cognitive cellular network is considered in which a secondary base-station (BS) operating in FD mode serves multiple uplink (UL) and downlink (DL) SUs operating in HD mode simultaneously. The spectrum is shared between secondary and primary networks, and thus uplink SUs and secondary BS generate interference on PUs. Sum-MSE is taken as the performance measure to design the transceivers. Under the impact of channel uncertainty, the robust minimization of the sum of mean squared-errors (MSE) of all estimated symbols subject to power constraints at the uplink SUs and secondary BS, and interference constraints projected to each PU is addressed.

Table of Contents

1. Introduction

The operation of Licensed Shared Access (LSA) systems has to be designed in a way that Quality-of-Service (QoS), in the form of spectral, energy and cost efficiency is guaranteed for both incumbent and licensee systems, when they have access to the spectrum. However, in order to achieve a joint, requested QoS objective, cooperation needs to characterize the operation between licensee operators/devices, as well as the concurrent transmissions of incumbent and licensee systems. For instance, since spectrum and resources such as antennas are expensive and, at the same time, cost efficiency constitutes a crucial factor for the successful deployment of an LSA system, cooperative techniques have to be designed towards such directions (section 5.1). Also importantly, cooperation can be realized by exchanging Channel State Information (CSI) of statistical nature between transmitters (section 5.2), as well as by synchronizing the Medium Access Control (MAC) frames of incumbent and sensing-based licensee networks (section 5.3). By means of synchronization and/or channel information exchange, interference mitigation techniques can be effectively developed, with the aim of increasing the throughput of two (or more) coexisting LSA systems. Limited feedback cooperation schemes can be designed to control interference and maximize the throughput while respecting the predefined constraints. The utilization of Opportunistic Beam-Forming (OBF) combined with Proportional Fair Scheduling (PFS) in the licensee network, in an LSA setup employing cooperation between the licensee (or Secondary System (SS)) and the incumbent (or Primary System (PS)) can boost the performance of the LSA system (section 5.4). In high speed train scenario, MIMO transmission techniques can be developed in which the excess multiple antennas over the spatial multiplexing are exploited to adequately suppress the ICI (section 5.5). LSA coordinated beamforming between incumbent and licensee cells can be developed to maximize a joint weighted sum utility function as an extension of traditional underlay cognitive radio approaches with interference temperature constraints (section 5.6). Full-duplex spectrum sensing system can be used to realize the simultaneous spectrum sensing and secondary transmission (section 5.7). Effective spectrum sharing between a collocated Multiple-Input-Multiple-Output (MIMO) radar that monitors the existence of a target and a wireless communications system can be proven to be feasible in a LSA system (section 5.8).Finally, under the impact of channel uncertainty, the robust minimization of the sum of mean squared-errors (MSE) of all estimated symbols subject to power constraints at the uplink SUs and secondary BS, and interference constraints projected to each PU in FD multi-user MIMO system that suffers from both self-interference and co channel interference can be addressed (section 5.9).

2. Purpose and Scope

In this deliverable, a number of algorithms and schemes that facilitate cooperative communication between entities belonging to a LSA network, is described, with reference to the investigated scenarios and use cases.

First, focusing on the small-cell/cloud-Radio Access Network (C-RAN) scenario, the case where a number of users requires a wireless service from a Virtual Mobile Network Operator (VMNO), is studied. More specifically, the VMNO rents antennas and spectrum from the existing C-RAN infrastructure and from the LSA network, respectively, with the aim of serving a number of

terminals. However, since the use of such resources is characterized by a cost, the VMNO has to select the appropriate number of antennas, along with an LSA bandwidth, such that the sum information rate per currency unit, is maximized. Motivated by the above situation, a cost efficiency metric is proposed, and then, based on that, as well as on the Zero-Forcing (ZF) distributed Multiple-Input-Multiple-Output (MIMO) precoding technique, we evaluate the optimal solution, in terms of cost efficiency, in comparison to an arbitrary, uncoordinated strategy. It is interestingly shown that the optimal scheme achieves a gain in cost efficiency, for a number of system scenarios.

In what follows, we investigate the operation of a Multiple-Input-Single-Output (MISO) macro-cell LSA system in the downlink. The system is composed of an incumbent Mobile Network Operator (MNO), which coexists with a licensee MNO, in the lack of any spectrum sensing procedure carried out at the latter. Given that framework, interference received by terminals assigned both to the incumbent and the licensee has to be efficiently controlled via precoding, as the goal is to maximize the average throughput of both systems, in terms of the achievable ergodic rate. Inspired by the underlay Cognitive Radio (CR) approach, we design a coordinated transmission scheme, which aims at maximizing the average rate of the licensee, subject to an average rate constraint for the incumbent. The coordination between the two LSA entities takes place under a realistic CSI regime, where each transmitter has mere access to the instantaneous direct link of its assigned user, while the rest of the channels are only statistically known via their covariance information. Such a CSI regime creates a formulation based on Team Decision theory, where the two decision makers (transmitters) have to solve the same optimization problem under different views of the global downlink channel. A novel set of applicable precoding schemes is proposed, based on Matched Filter (MF) and statistical ZF (sZF) solutions, and the two transmitters cooperate, in the lack of any exchange of instantaneous CSI. Coherent decisions are taken relying on statistical coordination criteria, and it is numerically shown that the proposed joint transmission scheme significantly outperforms the standard interference temperature-based underlay CR approach.

Additionally, we continue our focus on the macro-cell LSA scenario in the downlink and we also consider the existence of a Spectrum Sensing (SS) process that takes place at the licensee terminal. Influenced by both underlay (i.e., spectrum sharing) and interweave (i.e., opportunistic) CR systems, we analytically examine the throughput performance of a hybrid interweave/underlay MIMO LSA system. More concretely, we investigate the performance of hybrid LSA systems that switch between an interweave (i.e., egoistic) and an underlay (i.e., altruistic) transmission strategy, based on the SS results obtained, in the existence of combined instantaneous (for the direct channels) and statistical (for the cross-links) CSI at the transmitters (CSIT). The throughput performance of such a system is analytically examined by deriving novel closed form approximations describing the average achievable rate of the licensee as well as an expression describing the outage probability of incumbent communication. Exploiting the derived expressions, a new optimization problem is set up with respect to the SS parameters and then effectively solved, according to which the average rate of the licensee is maximized for a given outage constraint, imposed by the incumbent MNO. The throughput performance of the optimal SS design is numerically evaluated and compared to the performance achieved by the two standalone approaches, and significant average rate gains are illustrated.

Next, the uplink a macro-cell, hybrid LSA system is considered and the problem of jointly designing the SS parameters and the receive beamforming (BF) scheme, is tackled, in the presence of combined instantaneous and statistical CSIT, where the involved channels undergo correlated Rayleigh fading. As it has been described above, the goal of the proposed design is the maximization of the achievable average rate of the licensee, subject to an outage-related QoS constraint on incumbent communication. In order to formulate and then solve the problem, we derive novel closed form approximations, which describe the outage probability of the incumbent, both considering the hybrid approach as well as the standard opportunistic and spectrum sharing-based approaches. By means of simulation, it is shown that the designed hybrid LSA approach outperforms the optimized standard approaches, in terms of spectral efficiency for different outage probability levels as well as for different activity profiles of the incumbent.

We then consider the utilization of Opportunistic Beam-Forming (OBF) combined with Proportional Fair Scheduling (PFS) in the licensee network, in an LSA setup employing cooperation between the licensee (or Secondary System (SS)) and the incumbent (or Primary System (PS)) – which are both MNOs – so that the protection of the incumbent from interference is ensured. OBF is a scheme for downlink transmission in multi-antenna cellular systems that presents low feedback overhead, since it exploits Signal-to-Interference-plus-Noise-Ratio (SINR) values as a channel quality metric instead of full CSI. In the first considered use-case, we assume a setup comprised of two macro-cells, one belonging to the incumbent and the other belonging to the licensee, with an overlapping sector. A SINR threshold has been set for the PS. If a potential transmission of the SS would degrade the SINR of the scheduled Primary User (PU) below that threshold, the SS remains idle in that timeslot (TS). Then, the PS (which in that use-case utilizes also OBF in combination with PFS) can either serve the scheduled user or re-run PFS, which in the absence of interference from the SS will be based now on Signal-to-Noise-Ratio (SNR) feedback instead of SINR feedback. In the second use-case, we assume a setup comprised of a macro-cell belonging to the incumbent and three partially overlapping small-cells within a sector of that macro-cell belonging to the licensee. Only the small-cells employ OBF with PFS, while the macro-cell utilizes solely PFS. A SINR threshold has been set up for both the PUs and the Secondary Users (SUs). A cooperative transmission algorithm has been developed for the licensee system, which aims at finding the best n-tuple of small-cells to transmit at each TS (n = 0,…,3), so that the sum-rate throughput of the SS is maximized while at the same time the QoS threshold of the PS is respected. In both use-cases, numerical simulation results have shown that the proposed schemes boost the performance of the system.

We further consider the train scenario in which the high mobility leads to Intercarrier Interference (ICI) in OFDM communication systems. However, even at TGV speeds, it turns out that in a typical LTE setting, the channel time variation over an OFDM symbol duration can be adequately modelled by a linear variation. MIMO transmission techniques are then developed in which the excess multiple antennas over the spatial multiplexing are exploited to adequately suppress the ICI.

Next, we consider LSA coordinated beamforming between incumbent and licensee cells. Optimized beamforming techniques are introduced to maximize a joint weighted sum utility function. These techniques are furthermore extended to the case of partial CSIT, with a practical approximation of the ergodic sum utility function, which becomes exact in the Massive MIMO

setting. It is shown that this coordinated beamforming approach can be considered as an extension of traditional underlay cognitive radio approaches with interference temperature constraints.

Furthermore, we develop the full-duplex spectrum sensing system to realize the simultaneous spectrum sensing and secondary transmission. Firstly, the generalized expressions of the key sensing performance metrics are derived for multiple sensing antennas. Listen-and-talk protocol is applied and multiple sensing/transmission antennas are considered in this part. Secondly, the optimal decision threshold pair is investigated in order to minimize the total error rate of the system.

Next, we consider the problem of effective spectrum sharing between a collocated Multiple-Input-Multiple-Output (MIMO) radar that monitors the existence of a target and a wireless communications system. The target detection problem is reformulated using a sensing approach based on energy detection, while the BS applies beamforming to null the interference created at the radar receiver. Based on the theory of Hermitian quadratic forms and with the aid of the Linearly Constrained Minimum Variance (LCMV) beamforming solution, the performance of target detection, when the MIMO radar coexists with the data transmission is quantified and numerical results show that spectral coexistence is feasible.

Finally, we consider a FD multi-user MIMO system that suffers from both self-interference and co channel interference. The sum-MSE was taken as the performance measure to design the transceivers. Upper limits on both transmit power of the secondary UL users and BS, and interfering power at the PUs were considered. Accordingly, under the impact of channel uncertainty, we addressed the robust minimization of the sum of mean squared-errors (MSE) of all estimated symbols subject to power constraints at the uplink SUs and secondary BS, and interference constraints projected to each PU.

3. Reference Documents

1. Miguelez, E. Avdic, N. Marchetti, I. Macaluso, and L. Doyle, “Cloud-RAN Platform for LSA in 5G Networks - Tradeoff Within the Infrastructure”, in Proc. Of *6th International Symposium on Communications, Control and Signal Processing, Athens, Greece*, May 2014, pp. 522-525.
2. N. Marchetti, “Towards 5th Generation Wireless Communication Systems”, *ZTE Communications*, vol. 13, no. 1, pp. 11-19, March 2015.
3. M.C. Filippou, P. de Kerret, D. Gesbert, T. Ratnarajah, A. Pastore, and G. A. Ropokis, “Coordinated Shared Spectrum Precoding with Distributed CSIT”, *IEEE Transactions on Wireless Communications*, *in press*.
4. M.C. Filippou, G.A. Ropokis, D. Gesbert, and T. Ratnarajah, “Performance analysis and optimization of hybrid MIMO Cognitive Radio systems”, *in Proc. Of 2015 IEEE International Conference on Communication Workshop (ICCW)*, pp.555-561, 8-12 June 2015.
5. M.C. Filippou, G.A. Ropokis, D. Gesbert, and T. Ratnarajah, “Joint Sensing and Reception Design of SIMO Hybrid Cognitive Radio Systems”, *IEEE Transactions on Wireless Communications*, *in press*.
6. G.A. Ropokis, C.G. Tsinos, M.C. Filippou, K. Berberidis, D. Gesbert, and T. Ratnarajah, "Joint Power and Sensing Optimization for Hybrid Cognitive Radios with limited CSIT," in European Wireless 2015; *in Proc. of 21th European Wireless Conference*; pp.1-7, 20-22 May 2015.
7. N. Taramas, G. C. Alexandropoulos, and C. B. Papadias, “Opportunistic beamforming for secondary users in licensed shared access networks, *in Proc. IEEE International Symposium on Communications, Control and Signal Processing, Athens, Greece*, 21-23 May 2014.
8. K. Ntougias, N. Taramas and C. B. Papadias, “Low-feedback cooperative opportunistic transmission for dynamic licensed shared access,” *in Proc. 2015 European Signal Processing Conference (EUSIPCO 2015), Nice, France*, Aug. 31-Sept. 4, 2015.
9. Y. He, J. Xue, T. Ratnarajah and M. Sellathurai, “Full-duplex spectrum sensing for multi-antenna non-time-slotted cognitive radio networks,” in *IEEE International Workshop on Signal Processing Advances in Wireless Communications (SPAWC)*, Edinburgh, 3-6 July 2016.
10. F. Kaltenberger, A. Byiringiro, G. Arvanitakis, R. Ghaddab, D. Nussbaum,R. Knopp, M. Berbineau, Y. Cocheril, H. Philippe, and E. P. Simon, "Broadband wireless channel measurements for high speed trains," *in Proc. Of IEEE International Conference on Communications (ICC), London, UK*, June 2015.
11. K. Gopala and D. Slock, “MIMO OFDM Capacity Maximizing Beamforming for Large Doppler Scenarios,” *in Proc. Of IEEE International workshop on Signal Processing advances in Wireless Communications (SPAWC) Workshop*, Edinburgh, UK, 3-6 July, 2016.
12. K. Gopala and D. Slock, “High Doppler MIMO OFDM Capacity Maximizing Spatial Transceivers Exploiting Excess Cyclic Prefix,” *in Proc. SAS5G Workshop, ISWCS*, Poznan, Poland, Sept. 2016.

13. S.H. Muller-Weinfurtner, "Optimum Nyquist windowing in OFDM receivers," *IEEE Transactions on Communications*, Mar 2001.
14. C. Y. Ma, S.W. Liu, and C. C. Huang, "On optimum segment combining weight for ICI self-cancellation in OFDM systems under doubly selective fading channels," *in Proc. of Vehicular Technology Conference (VTC Spring)*, May 2012.
15. A. Farhang, N. Marchetti, L. E. Doyle, and B. Farhang-Boroujeny, "Low complexity CFO compensation in uplink OFDMA systems with receiver windowing," *IEEE Transactions on Signal Processing*, May 2015.
16. D.T.M. Slock, S. Valentin, and R. Chrabieh,"From network based location estimation to location aided communications", *Tutorial presented at 12th IEEE Int'l Symp. on Wireless Communication Systems (ISWCS)*, 25-28 Aug. 2015, Brussels, Belgium.
17. F. Negro, I. Ghauri, and D.T.M. Slock, "Deterministic Annealing Design and Analysis of the Noisy MIMO Interference Channel*," in Proc. IEEE Information Theory and Applications workshop (ITA), San Diego, CA, USA*, Feb. 2011.
18. F. Negro, D.T.M. Slock, and I. Ghauri, "On the Noisy MIMO Interference Channel with CSI through Analog Feedback," *in Int'l Symp. Comm's, Control and Sig. Proc. (ISCCSP), Rome, Italy*, May 2012.
19. Y. Lejosne, D. Slock, and Y. Yuan-Wu, "Foresighted Delayed CSIT Feedback for Finite Rate of Innovation Channel Models and Attainable NetDoFs of the MIMO Interference Channel," *in Proc. Wireless Days, Valencia, Spain*, Nov. 2013.
20. E.G. Larsson, O. Edfors, F. Tufvesson, and T.L. Marzetta, "Massive MIMO for Next Generation Wireless Systems," *IEEE Comm's Mag.,* Feb. 2014.
21. Y. Lejosne, M. Bashar, D. Slock, and Y. Yuan-Wu, "From MU Massive MISO to Pathwise MU Massive MIMO," *in Proc. IEEE Workshop on Signal Processing Advances in Wireless Communications (SPAWC), Toronto, Canada*, June 2014.
22. Y. Lejosne, M. Bashar, D. Slock, and Y. Yuan-Wu, "Decoupled, Rank Reduced, Massive and Frequency-Selective Aspects in MIMO Interfering Broadcast Channels," *in Proc. IEEE Int'l Symp. on Communications, Control and Sig. Proc. (ISCCSP), Athens, Greece*, May 2014.
23. W. Tabikh, D. Slock, and Y. Yuan-Wu, "The Pathwise MIMO Interfering Broadcast Channel," *in IEEE 16th Workshop Signal Proc. Advances in Wireless Comm's (SPAWC), 2015*.
24. W. Tabikh, K. Gopala, Y. Yuan-Wu, D. Slock, "From Multi-Antenna Underlay to LSA Coordinated Beamforming," *in Proc. SAS5G Workshop, ISWCS, Poznan, Poland*, Sept. 2016.
25. F. Negro, I. Ghauri, and D.T.M. Slock, "Sum Rate Maximization in the Noisy MIMO Interfering Broadcast Channel with Partial CSIT via the Expected Weighted MSE," *in IEEE Int'l Symp. on Wireless Commun. Systems (ISWCS), Paris, France*, Aug. 2012.
26. E. Yousif, F. Khan, T. Ratnarajah and M. Sellathurai, " On the Spectral Coexistence of Colocated MIMO Radars and Wireless Communications Systems," in Proc. of *IEEE International Workshop on Signal Processing Advances in Wireless Communications (SPAWC)*, Edinburgh, 3-6 July 2016.
27. ADEL deliverable D4.2

4. Abbreviations and Acronyms

5G	Fifth generation
AWGN	Additive White Gaussian Noise
BF	Beamforming
CFO	Carrier frequency offsets
CoBF	Coordinated Beamforming
CP	Cyclic Prefix
CR	Cognitive Radio
C-RAN	Cloud-Radio Access Network
CSI	Channel State Information
CSIR	Channel State Information at the Receiver
CSIT	Channel State Information at the Transmitter
DL	Downlink
ED	Energy Detection
ESIC-WSR	Expected Signal and Interference Covariance
EWSMSE	Expected Weighted Sum MSE
EWSR	Expected WSR
ExCP	Excess Cyclic Prefix
FDD	Frequency division duplexing
i.i.d.	Independent and identically distributed
ICI	Inter-carrier interference
LoS	Line-of-Sight
LSA	Licensed Shared Access
MAC	Medium Access Control
MaMIMO	Massive MIMO
MF	Matched Filter
MIMO	Multiple-Input-Multiple-Output
MISO	Multiple-Input-Single-Output

MNO	Mobile Network Operator
MU	Multi-User
NEWSR	Naive EWSR
OBF	Opportunistic Beam-Forming
OFDMA	Orthogonal frequency division multiple access
OOB	Out-of-Band
PFS	Proportional Fair Scheduling
QoS	Quality-of-Service
R-ZF	Regularized Zero-Forcing
RAN	Radio Access Network
Rx	Receive
SDMA	Spatial Division Multiple Access
SIMO	Single-Input-Multiple-Output
SISO	Single-Input-Single-Output
SINR	Signal-to-Interference-plus-Noise Ratio
SNR	Signal-to-Noise Ratio
sZF	Statistical Zero Forcing
SS	Spectrum Sensing and Secondary System
Tx	Transmit
TDD	Time division duplexing
VMNO	Virtual Mobile Network Operator
ZF	Zero Forcing

5. Exploiting Cooperation and Coordination for LSA Communications

5.1 Cost-efficient allocation of spectrum and antennas for the small-cell/C-RAN scenario

In the small cell/cloud RAN scenario, the ZF distributed MIMO technique has been investigated as precoding technique (this is related to the trade-off between the spectrum and the antennas associated with centralized resource allocation studied in Task T4.1).

5.1.1 Problem formulation

Let *K* users demand a wireless service from a VMNO. The operator rents antennas and spectrum from the C-RAN and the LSA system for the time needed to transmit the information. Using the C-RAN infrastructure (i.e., processing, backhaul, antennas) and LSA spectrum has a cost, in currency units per second. The aim of the network operator is to choose the optimal number of antennas, *M*, and bandwidth, *W*, such that the number of transmitted bits per currency unit is maximized. Fig. 1 shows the considered scenario.

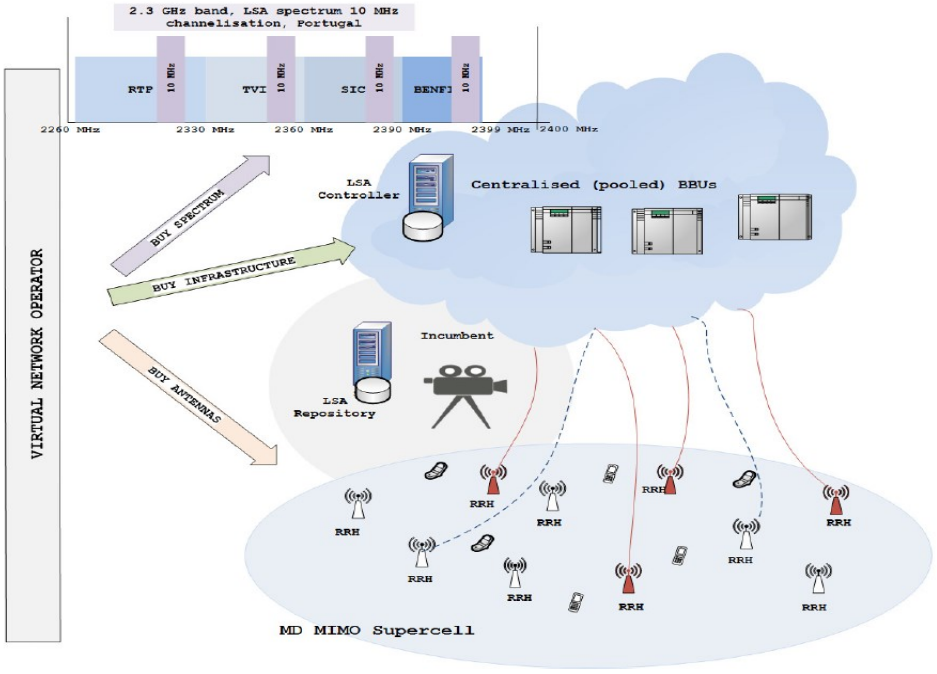

Fig. 1: C-RAN network deploying LSA sharing framework

Consider the downlink of a cloud-based MD-MIMO RAN with M_{max} available transmit antennas. The network operator chooses a subset of M antennas to transmit data to $K \le M \le M_{max}$ single-antenna users. The area covered by the M antennas is a super-cell. We assume the application of Spatial Division Multiple Access (SDMA), so that the K users access the whole bandwidth at the same time. The K data streams to each user are processed in the data center with ZF precoding and converted to M signals, which are transmitted to the antennas through an optical fiber network. The transmitted and received signals x and y are vectors of K elements, where the k^{th} element is the symbol transmitted and received at the k^{th} user antenna. The system model is:

$$\mathbf{y} = \mathbf{FHx} + \mathbf{n},$$

where $\mathbf{H} \in C^{MxK}$ and $\mathbf{F} \in C^{KxM}$ are the channel and precoding matrices, respectively and vector $\mathbf{n}$ is the complex Gaussian noise vector. Every symbol transmitted to every user has the same power, P, so that the total transmission power is KP. The power transmitted by each antenna depends on the precoding matrix $\mathbf{F}$. Without loss of generality, we neglect the per antenna power constraint.

Denote h_{km} the channel between the m^{th} transmit antenna and the k^{th} user. We consider a composite fading channel, i.e., $h_{km}(d_{km}) = \sqrt{\beta(d_{km})\sigma_{km}}w_{km}$, where $\beta(d_{km}) = \beta_0 d_{km}^{-\kappa}$ is the path loss as a function of the distance between the k^{th} user and m^{th} transmit antenna d_{km}. β_0 and κ are the signal loss at the reference distance and the path loss factor, respectively. $\sigma_{km} \ge 0$ is the large scale fading factor caused by shadowing and w_{km} is the small scale fading factor.

According to our model, if the k_{th} user's distance with the m_{th} antenna, d_{km} is an independent, identically distributed (i.i.d.) random variable, the entries of the channel matrix $\mathbf{H}$ are i.i.d., too. Let r_k be the power received by the k^{th} user. It can be shown that r_k is an i.i.d. random variable that can be approximated by an exponential distribution with average

$$\mathrm{E}\{r_k\} \sim P(M - K + 1).$$

Finally, the sum-rate capacity of the supercell is:

$$C = W \sum_{k=1}^{K} \log_2\left(1 + \frac{r_k}{N_0 W}\right),$$

where W is the bandwidth acquired from the LSA pool.

To serve K users, the service provider chooses M antennas and W MHz from the pool of resources offered by the cloud-based RAN and LSA. The spectrum cost, c_w, is the cost of using 1 MHz of bandwidth from the LSA for 1 s. The antenna cost, c_m, is the cost of using one distributed antenna for 1 s. The operative cost, c_o, is the cost of using the cloud infrastructure, e.g., backhaul and processing, for 1 s. The cost efficiency is the number of transmitted bits per cost unit (bits/cu) and is given as the ratio of the total rate to costs:

$$\eta(M,W)=\frac{W\sum_{k=1}^{K}\log\left(1+\frac{r_k}{N_0W}\right)}{c_mM+c_wW+c_o}$$

.

5.1.2 Key results

We consider the downlink of a cloud-based MD-MIMO RAN and we assume the application of SDMA, so that the users access the whole bandwidth at the same time. In Fig. 2, we compare the optimal cost efficiency with the efficiency obtained by an arbitrary strategy that either maximizes the number of antennas or the bandwidth. The results show that the optimal solution is able to transmit up to an order of magnitude more information for the same cost. The figure also shows that when the bandwidth cost is very small, maximizing the bandwidth is near-optimal. Similarly, if the bandwidth is expensive, the number of active antennas should be maximized.

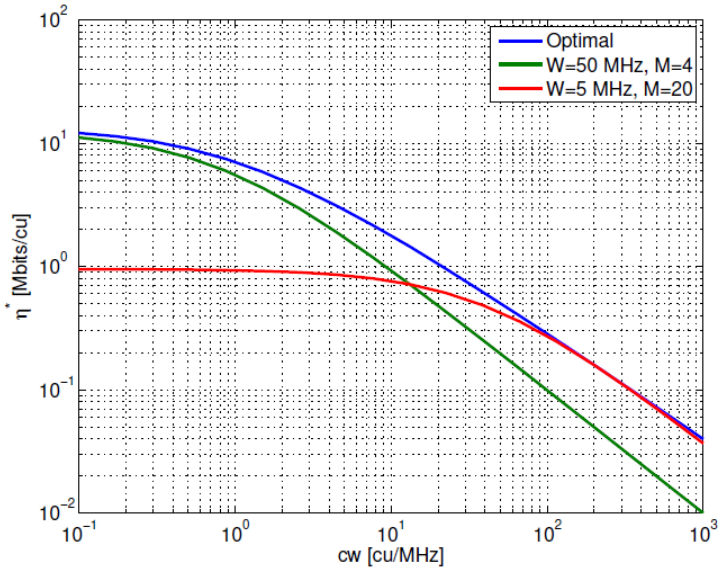

Fig. 2: Cost efficiency when the optimal spectrum and number of antennas are chosen, compared with the cost efficiency when the spectrum or the number of antennas are maximized.

5.1.3 Future work

In our future work, we consider a number of MVNOs with different capabilities accessing a shared C-RAN infrastructure. Some MVNOs are capable of modulating their signals with highly bandwidth efficient waveforms, while other MVNOs are using less bandwidth efficient technologies. In a C-RAN auction (involving antennas and spectrum) we will give lower values to the available bands that are right next to the incumbent in frequency domain. These bands have more stringent spectrum requirements in terms of out-of-band (OOB) emission than the ones further than incumbent's band. Therefore, MVNOs whose signals have lower OOB emissions than other MVNOs can more efficiently utilize bands close to the incumbent while reducing their cost. In this

study, we will consider the possibility of presence of MVNOs capable of using proposed waveforms for 5G. With such a heterogeneous mechanism, different MVNOs implicitly collaborate in a way to efficiently utilize the available band while minimizing their cost, and all utilize the underlying cooperative communication scheme, i.e. distributed ZF MIMO.

5.2 Statistically coordinated precoding with distributed CSIT for the macro-cell scenario

In this section, we focus on a MISO LSA system in the downlink, which consists of an incumbent MNO along with a licensee MNO. The two systems coexist and transmit simultaneously, thus, a SS task is not performed at the licensee side. Since a major objective of LSA systems is to guarantee QoS for all involved entities, the goal of a joint transmission design is the maximization of the average information rate of the licensee system, subject to the fact that the average rate of the incumbent lies above a given threshold (which depends on the service requirements of the incumbent terminal).

5.2.1 Problem formulation

The macro-cell MISO LSA system under investigation is illustrated in Fig. 3. It comprises of a multiple antenna incumbent transmitter, *TX* 1, which consists of M_1 antennas, along with its single-antenna assigned receiver, *RX* 1. Focusing on the downlink, the incumbent is willing to share the available spectrum with a MISO licensee system, comprising of a multiple antenna transmitter, *TX* 2, equipped with M_2 antennas, along with its single antenna assigned terminal, *RX* 2. Regarding the MISO channels involved, spatially correlated Rayleigh fading is assumed.

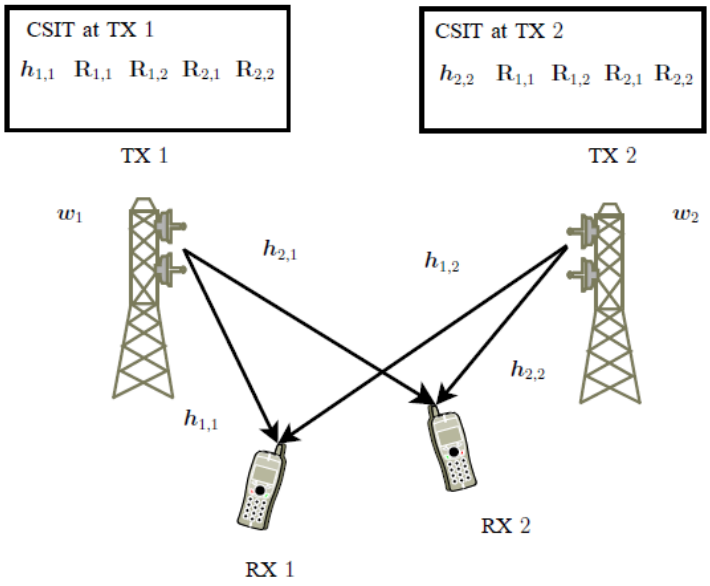

Fig. 3: The investigated MISO LSA network (downlink communication).

As far as the availability of CSIT is concerned, each of the transmitters has access to the instantaneous direct links of its assigned user (along with the corresponding covariance information), however, the interference links are merely known via their covariance matrices. The latter is a realistic assumption, since the second order statistics of these channels are slow varying in general and the covariance matrices can be exchanged between the transmitters through a low capacity/high delay backhaul link.

Given the described CSIT framework, the incumbent transmitter exploits the available combined channel information of the global downlink channel, in order to coordinate with the licensee transmitter, with the aim of maximizing the average rate of the latter, given a throughput constraint on incumbent communication. Thus, the optimization problem is the following:

$$\begin{aligned} &\left(\boldsymbol{w}_1^*, \boldsymbol{w}_2^*\right) = \arg\max \mathbb{E}\left[R_2\left(\boldsymbol{w}_1(\boldsymbol{h}_{1,1}), \boldsymbol{w}_2(\boldsymbol{h}_{2,2})\right)\right] \\ &\text{subject to } \mathbb{E}\left[R_1\left(\boldsymbol{w}_1(\boldsymbol{h}_{1,1}), \boldsymbol{w}_2(\boldsymbol{h}_{2,2})\right)\right] \geq \tau_1 > 0, \\ &0 \leq \|\boldsymbol{w}_1(\boldsymbol{h}_{1,1})\|^2 \leq P_1^{\max}, \;\; 0 \leq \|\boldsymbol{w}_2(\boldsymbol{h}_{2,2})\|^2 \leq P_2^{\max} \end{aligned}, \qquad \text{(P1)}$$

where $\mathbf{w}_1$, $\mathbf{w}_2$ are the two precoders that need to be optimized, $P_1^{\max}$, $P_2^{\max}$ stand for the maximum power levels at *TX* 1 and *TX* 2, respectively, and τ_1, is the threshold of the average rate of incumbent communication (which should be achievable, when *TX* 1 transmits with full-power MF BF, while *TX* 2 is silent).

5.2.2 Key results

The described optimization framework, falls within the paradigm of Team Decision theory, because both incumbent and licensee transmitters are actively engaged in cooperation, while being constrained by the locality of instantaneous CSIT. The following preliminary results will be proved useful in terms of solving an approximated version of optimization problem (P1), which is:

$$\begin{aligned} (\bar{P}_1^*, \boldsymbol{u}_1^*, \bar{P}_2^*, \boldsymbol{u}_2^*) = \arg\max \;\; & \mathbb{E}\left[\tilde{R}_2(\bar{P}_1, \boldsymbol{u}_1, \bar{P}_2, \boldsymbol{u}_2)\right] \\ & \text{subject to } \mathbb{E}\left[\tilde{R}_1(\bar{P}_1, \boldsymbol{u}_1, \bar{P}_2, \boldsymbol{u}_2)\right] \geq \tau_1 \\ & 0 \leq P_1 \leq P_1^{\max}, \;\; 0 \leq P_2 \leq P_2^{\max}, \\ & \|\boldsymbol{u}_1\| = 1, \;\; \|\boldsymbol{u}_2\| = 1. \end{aligned} \qquad \text{(P2)}$$

It should be noted that vectors $\mathbf{u}_1$ and $\mathbf{u}_2$ are the unit norm beamformers of *TX* 1 and *TX* 2, respectively and the new quantities describing the average ergodic rates are lower bounds of the ones appearing in problem (P1). The following two propositions are going to provide us with insights, in terms of finding a solution to problem (P2).

Proposition 1: The ergodic rate constraint of RX 1 is satisfied with equality by any optimal solution of problem (P2).

Proposition 2: An optimal solution of problem (P2) satisfies that either *TX* 1 or *TX* 2 transmits with full power.

Given these preliminary results, we design a new joint transmission scheme, which is a possible solution for problem (P1). Although it might be suboptimal, our approach guarantees that the incumbent rate constraint is satisfied in any case, and, as a result, it is a solution to problem (P1).

We start by deciding to restrict the search space to a definite set of joint precoding schemes. Hence, our approach consists of the following three steps:

- The precoding vector search space is based on MF and sZF BF solutions, thus, taking also into consideration Proposition 2, there are L=8 different joint precoding solutions to be evaluated.
- Having defined the elements of the set of potential joint BF solutions, focusing on each one of them, we find the (average) power levels for which the incumbent QoS constraint is satisfied with equality.
- After determining the power policies for which, for each element of the set, problem (P2) is feasible, we select the joint precoding/power allocation scheme that corresponds to the maximum average licensee rate.

With the aim of evaluating our novel joint transmission scheme, we numerically compare its throughput potential to the one obtained by the standard interference temperature-based underlay CR approach as well as to a performance outer bound, which would be obtained if the following problem would be solvable in practice:

$$\begin{aligned} \max_{\bar{P}_1,\bar{P}_2} \ & \mathbb{E}\left[\log_2\left(1+\frac{\bar{P}_2\|\boldsymbol{h}_{2,2}\|^2}{N_0+\bar{P}_1\lambda_{\min}\left(\mathbf{R}_{2,1}\right)}\right)\right] \\ \text{subject to} \ & \mathbb{E}\left[\log_2\left(1+\frac{\bar{P}_1\|\boldsymbol{h}_{1,1}\|^2}{N_0+\bar{P}_2\lambda_{\min}\left(\mathbf{R}_{1,2}\right)}\right)\right] \geq \tau_1, \\ & 0\leq\bar{P}_1\leq P_1^{\max},\ \ 0\leq\bar{P}_2\leq P_2^{\max}. \end{aligned} \qquad \text{(P3)}$$

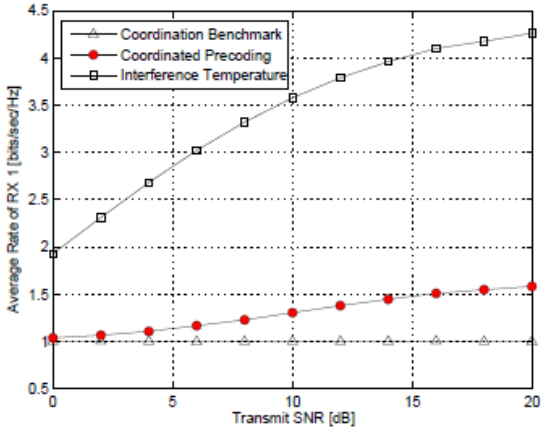

Fig. 4: Ergodic rate of RX 1 vs. transmit SNR, when incumbent QoS threshold τ_1 = 1bps/Hz.

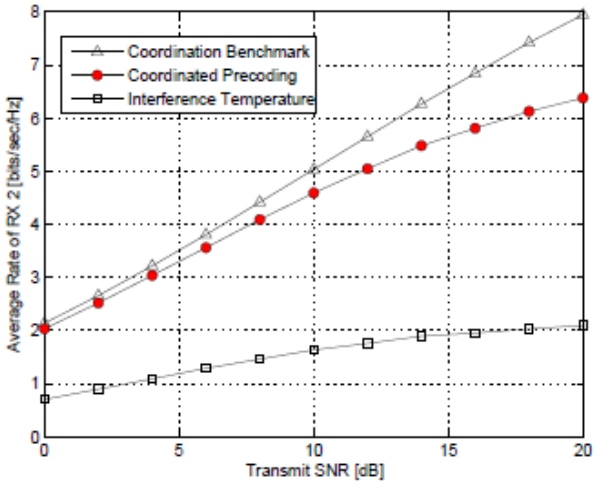

Fig. 5: Ergodic rate of RX 2 vs. transmit SNR, when incumbent QoS threshold τ_1 = 1bps/Hz.

In Fig. 4 and Fig.5, the average rates of *RX* 1 and *RX* 2, respectively, are plotted as a function of the system's transmit Signal-to-Noise Ratio (SNR) when $M_1 = M_2 = 4$ antennas. The involved curves correspond to the throughput performance of the novel designed joint precoding scheme, the interference temperature-based approach and the described performance outer bound.

One can observe that, focusing on the average rate performance of the licensee receiver, the coordination benchmark outperforms the other two schemes, however, the proposed approach is slightly inferior to it, especially for low transmit SNR regimes. At the same time, by observing Fig. 4, it is worth noticing that the QoS constraint on incumbent communication is satisfied by all three approaches, and this constraint is satisfied with equality by the outer bound.

5.2.3 Future work

In this work, we have focused on designing a joint precoding scheme for a spectrum sharing MISO LSA system, in the existence of local, combined instantaneous and statistical CSIT. The search space was confined into a finite number of strategies, where each one illustrates the major trade-off of maximizing the power of the direct link and minimizing the interference leakage towards the receiver of the counter-network. Approaching the global optimum is a very challenging task which can be tackled in the future. Also, the proposed scheme has strong potential in more complex systems, in the existence of multiple incumbent/licensee networks.

5.3 Sensing-dependent design of licensee transmission/reception: a joint optimization framework for the macro-cell scenario

In this section, we continue our study on multiple-antenna, macro-cell LSA systems, nevertheless, in contrast to section 5.2, the operation of the licensee system depends on the results of the Energy Detection (ED)-based SS process. Focusing on Half Duplex (FD) communication, we consider a degree of cooperation between the incumbent and the licensee system. This is

translated to the existence of synchronized Medium Access Control (MAC) frames, between the systems that form the LSA network. Given that system architecture, we design optimization algorithms, which aim at maximizing the spectral efficiency of the licensee system (when it decides to access the available spectrum), subject to outage-based constraints imposed by the incumbent MNO.

More specifically, in what follows:

- We start with deriving analytical expressions which describe the achievable average rate of licensee communication, as well as the outage probability of incumbent communication, with reference to a macro-cell MIMO LSA system in the downlink. Unlike standard interweave/underlay CR systems, we focus on a hybrid approach, according to which the licensee forms its transmission scheme according to the SS results obtained. Exploiting these expressions, we then formulate and solve, with respect to the SS parameters, the problem of maximizing the average rate of the licensee user, subject to an outage constraint on the incumbent terminal. Having derived the solution, we then compare our design to the optimal one for the corresponding standard interweave (i.e., opportunistic) and underlay (i.e., spectrum sharing) systems.
- Having completed our analysis in the downlink, we formulate a similar optimization problem in the uplink (i.e., a Single-Input-Multiple-Output (SIMO) system), where this time, the variables to be jointly optimized are: a). the SS parameters of ED (i.e., the sensing time and the ED threshold) and b). The receive BF vector (filter) at the multi-antenna licensee receiver. The conducted analysis takes place under a realistic CSI framework, where the direct links are known at the multiple antenna receivers, while covariance information is available for the interference channels (thus, introducing another dimension of cooperation between the two systems). Based on that framework, we derive a new closed form approximation for the outage probability of incumbent communication, which is proved useful in order to solve the described optimization problem.

In what follows, we start with examining the downlink of a macro-cell MIMO LSA system.

5.3.1 Downlink communication

5.3.1.1 Problem formulation

The downlink of a macro-cell MIMO LSA system is considered, that is composed of an incumbent transmitter, $TX1$ and its assigned incumbent receiver, $RX1$, along with a licensee transmitter, $TX2$ and its assigned receiver, $RX2$. It is assumed that each transmitter is equipped with M antennas, while each receiver is equipped with K antennas.

Regarding the availability of CSI at the two transmitters, since we focus on a MF based BF scheme, it is assumed that each transmitter, i, $i=1, 2$, has perfect knowledge of the direct channel towards its assigned user, i.e., $\mathbf{H}_{ii}$. Also, the channel between $TX2$ and $RX1$ is considered to be known both to $TX2$ and $RX2$. On the other hand, the MIMO interference link between $TX1$ and

RX 2 and the one between *TX* 1 and *TX* 2, are only statistically known to the two transmitters, thanks to the exchange of statistical information in a cooperative manner.

It is also supposed that an energy detection-based antenna selection algorithm is applied to both incumbent and licensee terminals, thus, in the remainder of this section, the involved MISO channels will be the resulting ones after antenna selection at the receiver side.

According to the time-slotted synchronized MAC frame model described earlier, each MAC frame of the licensee consists of (Fig. 6): a). a subframe devoted to ED-based SS, and its complementary, that is, b). a subframe during which data transmission takes place at TX 2.

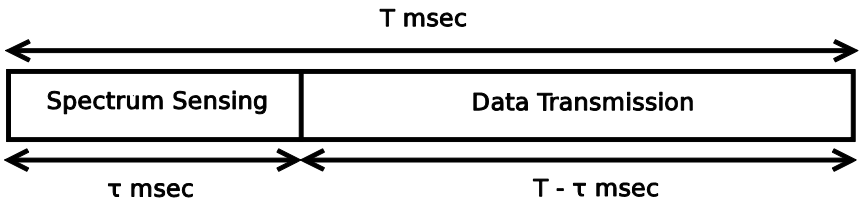

Fig. 6: MAC frame of the licensee system.

- SS subrame

By adopting MF BF at each transmitter, one can derive expressions for the false alarm probability, as well as for the average (over channel fading) detection probability. Assuming the transmission of symbols taken from a standard complex Gaussian codebook, these expressions are the following:

$$\mathcal{P}_{fa} = \mathcal{Q}\left(\sqrt{N}\left(\frac{\epsilon}{N_0} - 1\right)\right),$$

and

$$\mathcal{P}_{d,av} = \int_0^{\infty} \mathcal{P}_d(\beta_{00}) f_{\beta_{00}}(\beta_{00}) d\beta_{00}$$

Where ε is the ED threshold, N_0 is the variance of the Additive White Gaussian Noise (AWGN) and N is the number of SS samples, where $N = \tau f_s$. τ stands of the sensing time and f_s is the sampling rate for SS. Moreover, β_{00} denotes the power of the precoded incumbent signal, received by *TX* 2.

- Data transmission subframe

The achievable information rate for the hybrid LSA system is given by the following expression:

$$\mathcal{R}_{hyb} = \mathcal{R}_0 + \mathcal{R}_1$$

,

where the first term corresponds to the case where no incumbent activity is detected, as a result of SS, and the second term corresponds to the case where the incumbent is found to be active, by applying the ED SS algorithm.

The hybrid nature of the licensee transmission policy consists in the fact that when no incumbent activity is detected by means of SS, *TX* 2 transmits with a fixed power level, P_0, while, when this is not the case, it transmits with a power level P_1, where:

$$P_1 = \min\left\{\frac{\mathcal{I}}{|\mathbf{h}_{sp}\tilde{\mathbf{h}}_{ss}^H|^2}, P_s\right\}.$$

- Optimizing the SS parameters

The average rate-optimal (considering *RX* 2) values of the SS time and the ED threshold, for a target outage probability on incumbent communication, can be found by solving the following optimization problem:

$$(\epsilon^*, \tau^*) = \arg\max_{\epsilon,\tau} \quad \mathbb{E}\{\mathcal{R}_{hyb}\}$$
$$s.t. \quad \mathcal{P}_{out}^{hyb} = \mathcal{P}_t, \quad 0 < \tau \leq T, \quad \epsilon \geq 0, \quad \text{(P4)}$$

In order to solve problem (P4), closed form expressions (or at least closed form approximations) describing the average rate of the licensee receiver, as well as the outage probability of incumbent communication, have to be derived.

5.3.1.2 Key results

The incumbent system experiences an outage event, when, given that it is active, the Signal-to-Interference-plus-Noise Ratio (SINR) of *RX* 1 is below a target value, γ_0. Given that definition, we have concluded to the following proposition when $K = 2$ antennas at the receiver side:

Proposition 3: The outage probability of incumbent communication for a MIMO hybrid macro-cell LSA system, with K = 2 and energy-based antenna selection at each receiver, is given by the following expression:

$$\mathcal{P}_{out}^{hyb} = \mathcal{P}_{out,0} + \mathcal{P}_{out,1},$$

where the first term depends on the occurrence of the event in which the licensee finds no incumbent activity, by applying SS, whereas the second term corresponds to its complementary event. The two terms can be found in closed form.

Regarding the average rate of RX 2, this can be found in closed form by starting with the following equation:

$$\mathbb{E}\{\mathcal{R}_{hyb}\} = \mathbb{E}\{\mathcal{R}_0\} + \mathbb{E}\{\mathcal{R}_1\}$$

where, by exploiting the distributions of the involved channels (i.e., i.i.d. Rayleigh fading), a closed form approximation can be found.

Given the above results, one can solve optimization problem (P4) by applying an exhaustive search over the number of SS samples, N, which belongs to the discrete number set $\{1, \ldots, Tf_s\}$, where T corresponds to the duration of a licensee MAC frame. Each time, an appropriate value for ED threshold, ε, can be found with bisection, in order to fulfil the incumbent outage probability constraint with equality.

With the aim of evaluating our design, extensive Monte Carlo simulations have been performed, with the aim of cross-validating the correctness of the closed form expressions found. On top of that, comparisons have been made with the rate-optimal designs of the corresponding standalone interweave and underlay systems.

In Fig. 7, the ergodic rate of the licensee receiver is depicted as a function of the outage probability constraint, when the incumbent is active for 30% of the time.

It is more than evident that the validity of the theoretical expressions can be proved by the convergence of the Monte Carlo curves to the theoretical ones. What is more, the proposed rate-optimal hybrid design, significantly outperforms the standard approaches. Furthermore, it can be observed that as the outage probability constraint become stricter, the corresponding average rate of the licensee is reduced. This happens because, as the incumbent tolerates less interference on average, the licensee has to transmit primarily with the aim of protecting incumbent transmissions.

In Fig. 8, the same quantities are illustrated when the incumbent is busy for 70% of the time. The same phenomena as in Fig. 7 can be observed, with the exception being in that the standard underlay approach outperforms the interweave one, for the whole examined outage probability interval.

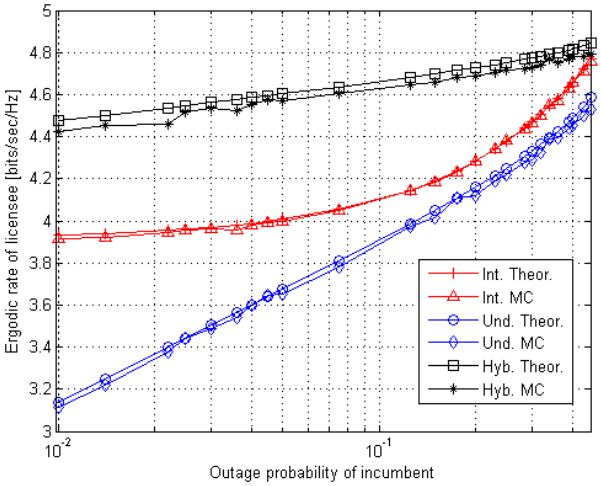

Fig. 7: Ergodic rate of licensee vs. outage probability of incumbent, incumbent active for 30% of the time.

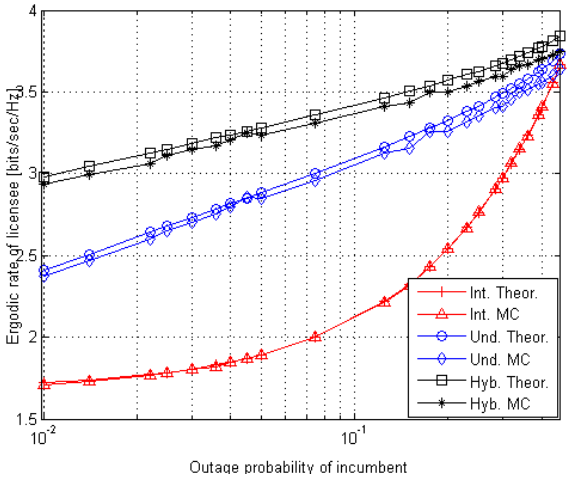

Fig. 8: Ergodic rate of licensee vs. outage probability of incumbent, incumbent active for 70% of the time.

5.3.1.3 Future work

We have analytically investigated the performance analysis of a hybrid interweave/underlay macro-cell MIMO LSA system with antenna selection at the receiver side, and we have optimized the SS parameters towards maximizing the spectral efficiency of the licensee system, given a QoS-based constraint on incumbent communication. Interesting extensions can be made in terms of investigating the existence of multiple incumbent and licensee MNOs, where the latter will conduct collaborative SS.

5.3.2 Uplink communication

5.3.2.1 Problem formulation

The uplink of a hybrid interweave/underlay macro-cell LSA system is considered, as shown in Fig. 9, which comprises of a single antenna transmitter of a licensee network, *TX* p, that communicates with a multiple-antenna receiver, *RX* p. It is assumed that the incumbent MNO is willing to share part of its spectral resources with a licensee network. The latter is composed of a single-antenna transmitter, *TX* s, communicating with a multiple antenna receiver, *RX* s. In what follows, it is assumed that *RX* p and *RX* s are equipped with *M* antennas, each. (In [6] a similar system has been investigated, however, in the existence of uncorrelated channels.)

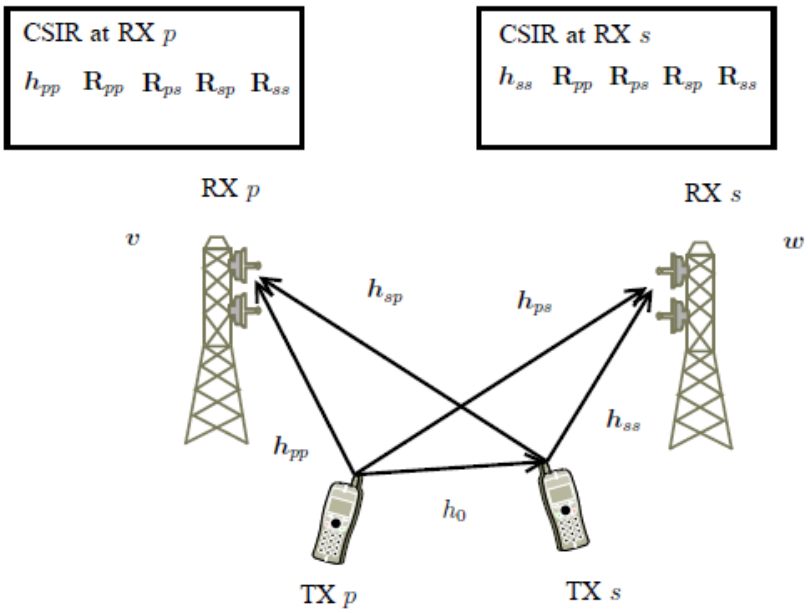

Fig. 9: The examined hybrid LSA network (uplink communication).

It is also assumed that channel vectors $\mathbf{h}_{mn}$, where m,n belong to the set {p,s} are spatially correlated, or:

$$\boldsymbol{h}_{mn} = \mathbf{R}_{mn}^{\frac{1}{2}} \boldsymbol{h}_{mn,w}, \quad m,n \in \{p,s\},$$

where $\mathbf{R}_{mn}^{1/2}$ is the symmetric square root of covariance matrix $\mathbf{R}_{mn}$ of SIMO channel $\mathbf{h}_{mn}$ and $\mathbf{h}_{mn,w}$ is a vector the elements of which are i.i.d. complex normal random variables.

Focusing on the availability of CSI at the receiver (CSIR), a practical scenario is considered, according to which RX i, i ∈ {p, s}, is aware of direct channel $\mathbf{h}_{ii}$, while it merely has statistical knowledge of the global uplink channel, in the form of covariance information. Since such information is slow varying, as it has been mentioned before, it can be available at each of the RXs via a low capacity/high latency feedback link.

- Description of the SS phase

It is assumed that the licensee MAC frame is the one shown in Fig. 6. As a result, by assuming the application of ED for SS at *TX*s and by properly applying the central limit theorem, given that the inputs are complex normal random variables, we obtain the following expressions, which describe the probability of false alarm and the probability of detection:

$$\mathcal{P}_f(N,\varepsilon) = \mathcal{Q}\left(\sqrt{N}\left(\frac{\varepsilon}{N_{0,0}} - 1\right)\right),$$

and

$$\mathcal{P}_d(N,\varepsilon) = \mathcal{Q}\left(\sqrt{N}\left(\frac{\varepsilon}{P_p\sigma_0^2 + N_{0,0}} - 1\right)\right),$$

respectively, where $N_{0,0}$ denotes the noise power at *TX* s, σ_0^2 denotes the variance of the Single-Input-Single-Output (SISO) channel between *TX* p and *TX* s, and, as mentioned before, N is the number of SS samples and ε the ED threshold.

- Description of the data transmission phase

Since we focus on a hybrid licensee system, where the receiver is designed according to the SS results, the instantaneous information rate of RX s, will be a sum of two terms, one for each SS result (i.e., when the total energy of the samples is higher than the threshold ε, and when it is lower than that). Hence, for each of these terms, we have:

$$\mathcal{R}_k = \alpha_k \log_2\left(1 + \frac{\left|\boldsymbol{w}_k^{\mathrm{H}}\boldsymbol{h}_{ss}\right|^2 P_k}{N_{0,s}}\right) + \beta_k \log_2\left(1 + \frac{\left|\boldsymbol{w}_k^{\mathrm{H}}\boldsymbol{h}_{ss}\right|^2 P_k}{N_{0,s} + \left|\boldsymbol{w}_k^{\mathrm{H}}\boldsymbol{h}_{ps}\right|^2 P_p}\right),$$

where, P_k, $k = 0,1$, is the transmit power of *TX* s, when each of the two SS-related events occurs, $\mathbf{w}_k$ is the applied receive BF vector at *RX* s and $N_{0,s}$ stands for the noise power at *RX* s. Parameters α_k and β_k, are given by:

$$\alpha_0 = \frac{T-\tau}{T}\mathcal{P}_0\left(1-\mathcal{P}_f\right), \quad \beta_0 = \frac{T-\tau}{T}\mathcal{P}_1\left(1-\mathcal{P}_d\right),$$
$$\alpha_1 = \frac{T-\tau}{T}\mathcal{P}_0\mathcal{P}_f, \quad \beta_1 = \frac{T-\tau}{T}\mathcal{P}_1\mathcal{P}_d,$$

Assuming that *TX* p transmits with a fixed power level, P_p and that *RX* p applies a MF-based receive BF vector, $\mathbf{v}$, we formulate the problem of maximizing the average rate of licensee communication, given an outage-based constraint for incumbent communication. The parameters to be optimized are: a). The SS parameters N and ε, as well as b). The receive BF vector $\mathbf{w}_1$ (we assume that $\mathbf{w}_0$ is the MF-based solution, as no incumbent activity is detected as a result of SS) and c). The power level P_1. The investigated optimization problem can be formally expressed as follows:

$$\begin{aligned} \underset{\boldsymbol{w}_1\in\mathbb{C}^{M\times 1},\tau,\varepsilon,P_1}{\text{maximize}} \quad & \mathbb{E}_{|\boldsymbol{h}_{ss}}\{\mathcal{R}\} \\ \text{subject to} \quad & \mathcal{P}_{\text{out}} \le \tilde{\mathcal{P}}_{\text{out}}, \;\; \mathcal{P}_d = \tilde{\mathcal{P}}_d, \;\; \|\boldsymbol{w}_1\| = 1, \\ & 0 < P_1 \le P_{\text{peak}}, \;\; 0 < \tau \le T, \;\; \varepsilon \ge 0, \end{aligned} \qquad \text{(P5)}$$

where P_{peak} is a peak power level at *TX* s.

5.3.2.2 Key results

Solving problem (P5) is a cumbersome task, thus, the following assumptions can be made in order to conclude to a solution to a simpler, approximate problem:

a. A lower bound of the objective function can be found in closed form and
b. We focus on an interference-limited (i.e., high Interference-to-Noise Ratio (INR)) scenario, where interference is the main source of signal degradation, as compared to noise.

It should be noted that closed form approximations describing the outage probability of incumbent communication and a lower bound of the average licensee rate can be found (see the analysis in [5]). Given these results, an alternating, iterative algorithm of jointly optimizing the SS parameters and the receive BF policy applied at *RX* s, can be applied. The algorithm, is the one that follows:

Algorithm Jointly optimizing BF vector $\mathbf{w}_1$ and SS parameters τ and ε

Step 1 (initiation): Fix the receive BF scheme such that $\mathbf{w}_1 = \mathbf{w}_1^{(0)}$ and increase counter by one.

Step 2: For the *n*-th iteration solve an approximate version of (P5) by fixing $\mathbf{w}_1 = \mathbf{w}_1^{(n-1)}$ and find values τ_n and ε_n.

Step 3: Exploiting values τ_n and ε_n solve an approximate problem of (P5) and determine receive BF vector $\mathbf{w}_1^{(n)}$.

Step 4: Compute the value of the objective, denoted by C_n.

Step 5: Increase the counter by one and the absolute difference of values C_n and C_{n-1} is smaller than an arbitrary small positive number ξ, when n >1, stop, otherwise go to Step 2.

Note 1: Regarding the transmit power level of TX s, this can be easily determined by bisection, focusing on the closed form approximate expression that describes the outage probability of incumbent communication.

Note 2: It is worth emphasizing the fact that cooperation between the licensee transmitter and the licensee receiver exists, in terms of solving the optimization problem, as the updated SS parameters (in each step of the algorithm) are exchanged between *TX* s and *RX* s.

Having solved the formulated optimization problem, we numerically evaluate its performance, by comparing it with the one achieved by the optimized, standard interweave and underlay LSA systems. In order to formulate the channel covariance matrices, the exponential antenna correlation model is adopted, which is characterized by the spatial antenna correlation factor, $0< \rho <1$.

In Fig. 10, we evaluate the quality of the closed form approximation of a probability involved in the expression of the incumbent outage probability (see [5]), as a function of parameter γ_0, which is the SINR threshold, below which an outage event is declared at *RX* p. As it can be observed, the approximation is satisfactory for both values of the antenna correlation factor, especially when ρ is small.

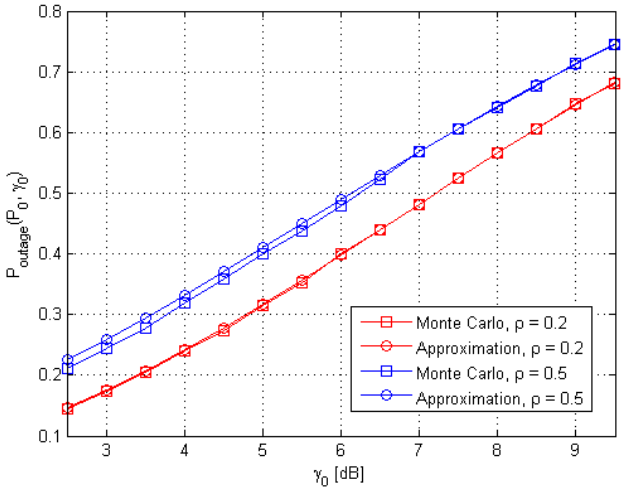

Fig. 10: Quality of approximating probability $P_{outage}(P_0, \gamma_0)$ for different values of γ_0.

In Fig. 11, the achievable average rate of *RX* s is illustrated for the three optimized systems (i.e., the hybrid, as well as the standard interweave and underlay ones), as a function of the activity profile of the incumbent system, when the outage constraint of the incumbent is equal to 2%. One can observe that the designed hybrid LSA system outperforms the standard systems for the whole incumbent activity profile range. Also importantly, it is interestingly observed that the average rate of RX s, regarding the hybrid LSA system, balances between two extremes: for low incumbent activity profiles it converges to the average licensee rate achieved by the interweave LSA system, while, when the incumbent is almost constantly in transmission mode, it converges to the throughput performance of the underlay LSA system.

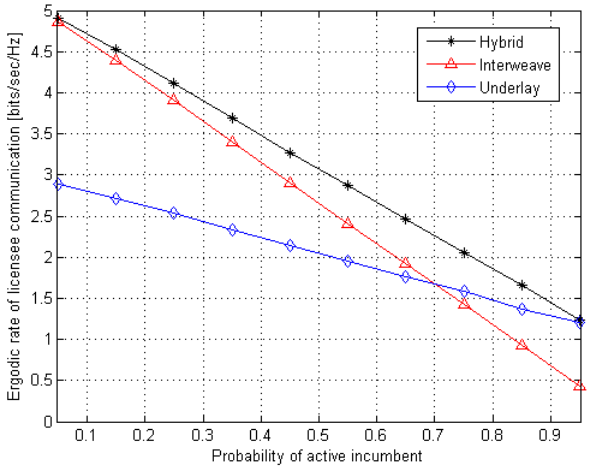

Fig. 11: Ergodic rate of *RX* s vs. incumbent activity profile, outage probability constraint: 2%.

5.3.2.3 Future work

In this section, it has been shown that the optimized hybrid SIMO LSA system outperforms the equivalent, optimized interweave and underlay systems, in terms of spectral efficiency. Interesting extensions can be made regarding the existence of multiple licensee operators (or transmitter/receiver pairs).

5.4 Opportunistic beamforming for LSA licensee networks

Opportunistic beamforming (OBF) has been proposed as a low feedback transmission scheme for the downlink (DL) of cellular systems equipped with multi-antenna base stations (BS). This communication method exploits the inherent multi-user diversity (MU-Div) of such setups to schedule the user with the most favorable instantaneous channel quality. Typically, OBF is applied jointly with a scheduling algorithm.

In this work, we utilize OBF with joint scheduling in settings that involve simple cooperation schemes between an incumbent and a licensee system by applying licensed shared access (LSA)-type rules. Thus, non-orthogonal sharing of the spectrum between these entities is enabled in an efficient manner.

We focus on a horizontal spectrum sharing scenario, where both of the aforementioned stakeholders are mobile network operators (MNO). This use case is considered as an additional business model under the context of the advanced LSA paradigm envisaged in the ADEL project. However, the described framework is generic and can be applied, in principle, in conventional vertical spectrum sharing scenarios as well (taking into account the minor modifications required in the setup of the incumbent) – e.g., use cases wherein the incumbent is a military radar or a wireless microphone.

First, we study the performance of a setup comprised by two homogeneous systems – more specifically, by two macro-cell BSs (MBS), where the one belongs to the incumbent and the other to the licensee. The standard proportional fair scheduler (PFS) is considered in this case. Then, we investigate (a) the impact of the power levels according to the spectrum sharing requirements, and (b) the performance of the system when a new delay-constrained maximum PFS is employed. In the scenarios considered so far, the established spectrum sharing rules protect the incumbent from harmful interference but they do not provide any quality-of-service (QoS) guarantees to the licensee. Finally, we turn our attention into a system where a certain QoS level is ensured for both entities, as it is required in LSA. In the latter use case, the composite system is heterogeneous, with the licensee system being comprised of three small-cell BSs (SBS). A simple cooperation scheme that involves minimal signaling overhead is described. The numerical simulations reveal that despite its simplicity, this approach presents considerable performance gains over non-cooperative systems, in terms of the achieved data rates and sum-rate (SR) throughput.

The motivation behind this work was to gain insight about how various parameters (e.g., dimensioning, scheduler, spectrum sharing rules, cooperation scheme) affect the behavior and performance of a spectrum sharing system.

5.4.1 Joint OBF with PFS in Spectrum Sharing Setups

System Setup and Operation

Initially, we consider two MBSs sharing a common sector, as shown in Fig. 12. The incumbent and the licensee MBS have the same transmission power and cell radius and are equipped with the same number of transmit antennas. A signal-to-interference-plus-noise (SINR) threshold γ_{Th}^{Inc} has been set for the users of the incumbent, as a QoS target, and reported to the licensee's MBS. Moreover, it is assumed that the two systems are perfectly synchronized.

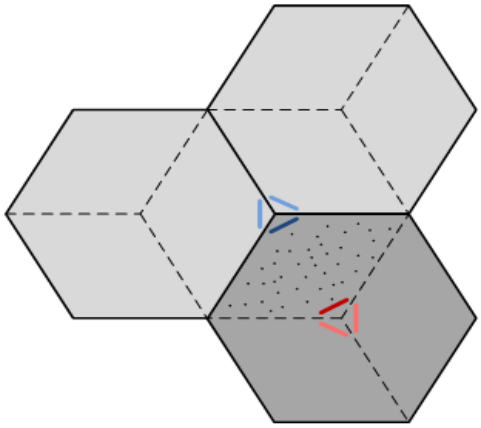

Fig. 12: Topology of the considered setup.

The operation of the composite system is divided in two phases: In the scheduling phase, each MBS selects a single user according to the OBF with PFS mechanism. In the transmission phase, the incumbent's MBS serves its scheduled user, while the licensee's MBS transfers data to its selected user only if this potential transmission would not drop the SINR of the incumbent's scheduled user below the predefined threshold level; otherwise, it remains idle during this timeslot (TS). In the latter case, the incumbent's MBS can rerun the scheduling process in order to select the preferable user based on signal-to-noise-ratio (SNR) feedback instead of SINR reports.

Signal and Channel Models

We adopt the notation BS_l ($l=1, 2$), where $l=1$ is used to denote the incumbent's MBS and $l=2$ is used for the licensee's MBS. Similarly, the transmit power of each BS and the corresponding cells are denoted as P_l and cell_l, respectively, with $P_1=P_2=P$. All BSs are equipped with $N_t=4$ antennas and wish to communicate with their scheduled user. Each user utilizes a terminal device equipped with a single omni-directional antenna, i.e., $N_r=1$. This is a realistic assumption, since in practice it is difficult to place multiple antennas at a user terminal (UE) due to cost, size, and power consumption constraints. Thus, a (4×1)-MISO (multiple-input single-output) channel is formed between a MBS and a mobile user (MU) at the DL. We assume a user population of $2K$ mobile users MU_k $(k=1, \ldots K$ randomly placed in the common sector between the incumbent and the licensee MBS, where half of them belong to the incumbent $(k=1, \ldots K$ and the other half belongs to the licensee $(k=K+1, \ldots K$.

Let $\mathbf{h}_{k,l} \in \mathrm{C}^{1\times N_t}$ ($k = 1, \ldots K$, $l = 1, 2$ and C denote the set of complex numbers) be the complex channel vector between MU_k and BS_l. A block fading channel model is assumed, such that $\mathbf{h}_{k,l}$ remains constant over timeslots of duration T samples. The baseband received signals at each TS for the scheduled user of the incumbent and the licensee are expressed as follows:

$$y_k^{\mathrm{Inc}}(t) = \underbrace{\sqrt{P_1}\mathbf{h}_{k,1}(t)\mathbf{X}_1(t)}_{\text{desired signal}} + \underbrace{\sqrt{P_2}\mathbf{h}_{k,2}(t)\mathbf{X}_2(t)}_{\text{interference}} + \underbrace{n_k(t)}_{\text{noise}}, \tag{1}$$

$$y_k^{\mathrm{Lic}}(t) = \underbrace{\sqrt{P_2}\mathbf{h}_{k,2}(t)\mathbf{X}_2(t)}_{\text{desired signal}} + \underbrace{\sqrt{P_1}\mathbf{h}_{k,1}(t)\mathbf{X}_1(t)}_{\text{interference}} + \underbrace{n_k(t)}_{\text{noise}}, \tag{2}$$

where $\mathbf{X}_l(t) \in \mathrm{C}^{N_t\times T}$ ($l = 1, 2$) are matrices containing T transmitted symbols in timeslot t for BS_l, and $n_k(t) \in \mathrm{C}^{N_t\times T}$ is a zero-mean additive white Gaussian noise (ZM-AWGN) vector with covariance matrix $\sigma_k^2\mathbf{I}_T$, where $\mathbf{I}_T$ is the $T\times T$ identity matrix.

The corresponding SINR values are given by:

$$\gamma_k^{\mathrm{Inc}}(t) = \frac{P_1\left\|\mathbf{h}_{k,1}(t)\right\|^2}{P_2\left\|\mathbf{h}_{k,2}(t)\right\|^2 + \sigma_k^2} \tag{3}$$

$$\gamma_k^{\mathrm{Lic}}(t) = \frac{P_2\left\|\mathbf{h}_{k,2}(t)\right\|^2}{P_1\left\|\mathbf{h}_{k,1}(t)\right\|^2 + \sigma_k^2} \tag{4}$$

When $\gamma_k^{\mathrm{Inc}}(t) < \gamma_{Th}^{\mathrm{Inc}}$, the licensee's MBS is not allowed to transmit. Then, the baseband received signal at the scheduled user of the incumbent is given by

$$y_k^{\mathrm{Inc}}(t) = \underbrace{\sqrt{P_1}\mathbf{h}_{k,1}(t)\mathbf{X}_1(t)}_{\text{desired signal}} + \underbrace{n_k(t)}_{\text{noise}} \tag{5}$$

and the corresponding SINR reduces to SNR:

$$\gamma_k^{\mathrm{Inc}}(t) = \frac{P_1\left\|\mathbf{h}_{k,1}(t)\right\|^2}{\sigma_k^2}. \tag{6}$$

The elements of $\mathbf{h}_{k,l}$ are assumed to be independent zero-mean complex Gaussian random variables (RVs) with variance

$$a_{k,l}^2 = \underbrace{PL_{\mathrm{ref}}^l\left(\frac{d_{k,l}}{d_{\mathrm{ref}}^l}\right)^{-\Gamma}}_{\text{Path Loss}} \cdot \underbrace{s_{k,l}}_{\text{Shadowing}} \cdot \underbrace{g_{k,l}}_{\substack{\text{Normalized}\\ \text{direction-based}\\ \text{antenna response}}}, \tag{7}$$

where PL_{ref}^{l} is the path loss at some reference distance d_{ref}^{l} from BS_l, $d_{k,l}$ is the distance between MU_k and BS_l, Γ is the path loss exponent which is defined as:

$$\Gamma = \begin{cases} 0 & d_{k,l} < 30\text{m} \cdot r_l \\ 2 & 30\text{m} \cdot r_l \le d_{k,l} \le d_{\text{ref}}^{l} \cdot r_l \\ 3.7 & d_{k,l} > d_{\text{ref}}^{l} \cdot r_l \end{cases}, \tag{8}$$

where r_l is the radius of cell_l (1Km for both MBSs), $s_{k,l} = 10^{S/10}$ is a log-normal RV which represents shadow fading with standard deviation $S = 8$ dB and $g_{k,l}$ is the normalized direction-based antenna response of BS_l, see [1]. We assume a parabolic response model, which is given (in dB) by

$$g_{k,l}\left(\theta_{k,l} - \omega_l\right) = \max\left\{-12\left(\frac{\theta_{k,l} - \omega_l}{\Theta}\right)^2, A_s\right\} \tag{9}$$

In Eq. (9), $\theta_{k,l}$ is the direction of MU_k with respect to the location of BS_l, ω_l is the beam direction of BS_l, $\Theta = 70\pi/180$ is the 3-dB beamwidth of the response, and $A_s = -20\text{dB}$ is the sidelobe level of the response.

Joint OBF with PFS

At each TS, each base station BS_l transmits its own pilot signal by selecting a beam in a pseudo-random manner from the fixed predetermined set of beams, as in the case of transmitting a data signal. Then, each mobile user MU_k estimates $\mathbf{h}_{k,l}$ for the current selection of beamforming weights and feeds back to its corresponding BS_l its estimated SINR $\gamma_k(t)$ or, equivalently, its requested data rate $R_k(t)$ (i.e., the data rate that the channel can currently support), which is given by Shannon's capacity formula

$$R_k(t) = \log_2\left[1 + \gamma_k(t)\right] \tag{10}$$

The BS scheduler keeps track of the average throughput of each user $T_k(t)$ in a sliding window of the past with length W timeslots and schedules the MU_k user with the largest ratio $R_k(t)/T_k(t)$ (i.e., the one whose rate is near to its own peak, according to the service history). The BS updates the average throughputs at each TS according to the following exponential-smoothing formula:

$$T_k(t+1) = \begin{cases} \left(1 - \frac{1}{W}\right)T_k(t) + \frac{R_k(t+1)}{W}, & k = k^* \\ \left(1 - \frac{1}{W}\right)T_k(t), & k \ne k^* \end{cases}, \tag{11}$$

where k^* denotes the scheduled user.

When the number of users is large, OBF performs almost optimal beamforming per-user despite the absence of channel state information at the transmitter (CSIT).

5.4.2 Key Results

Computer simulation results have a) shown that the proposed technique exploits MU-Div and boosts the SR throughput of the coexisting systems and b) revealed the trade-off between the incumbent's network QoS requirement and the overall LSA system's throughput. I particular, assuming transmit power over noise variance ratio $P = 15$ dB and $W = 50$ TS, the performance of the system is demonstrated in Fig. 13 for $\gamma_{Th}^{\text{Inc}} = 5$ and 10 dB, where it is observed that:

- The average system throughput R_s increases with increasing number of MUs K up to a maximum value.
- R_s improves also with decreasing SINR threshold γ_{Th}^{Inc}. Conversely, higher QoS requirement leads to lower R_s.
- The additional control phase for the incumbent's BS when the licensee's BS remains idle slightly improves R_s. However, in Fig. 13 we have not taken into account the throughput loss that will be encountered in practice due to the additional time spent for the rescheduling process.

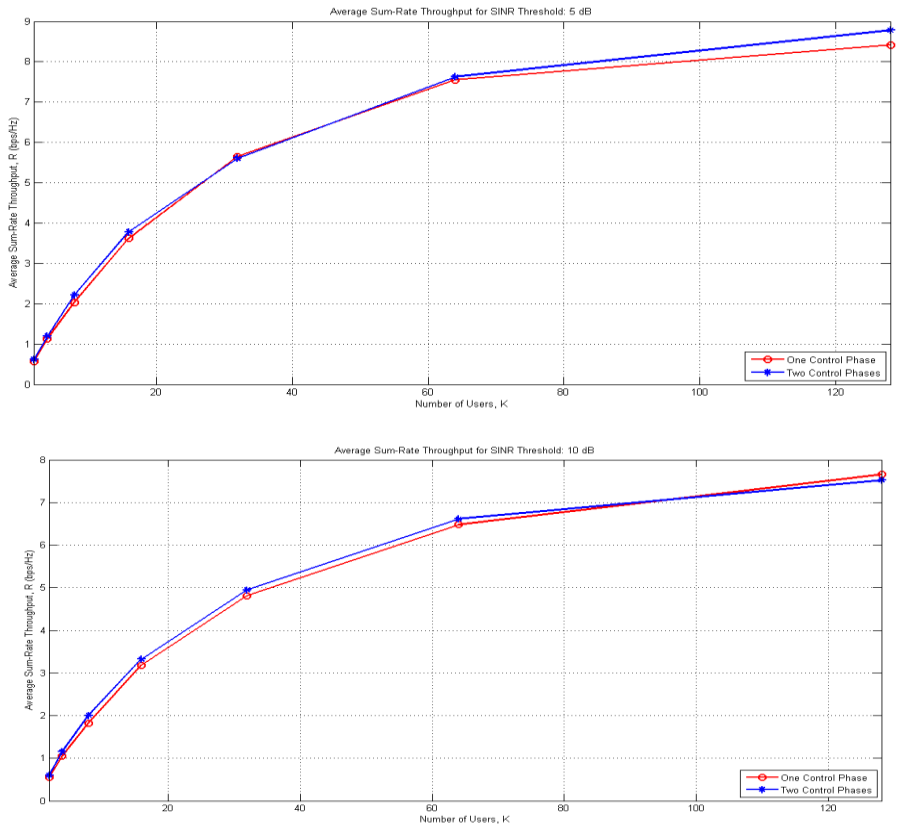

Fig. 13: Average system throughput R_s versus the number of mobile users K for transmit power over noise variance ratio P = 15 dB for both incumbent and licensee BS and different SINR thresholds.

In Fig. 14 the percentage of the licensee system's blocked transmissions for various SINR thresholds is depicted and it is observed that:

- As the number of users increases, the percentage of blocked transmissions decreases.
- Similarly, this performance metric improves with decreasing SINR threshold.

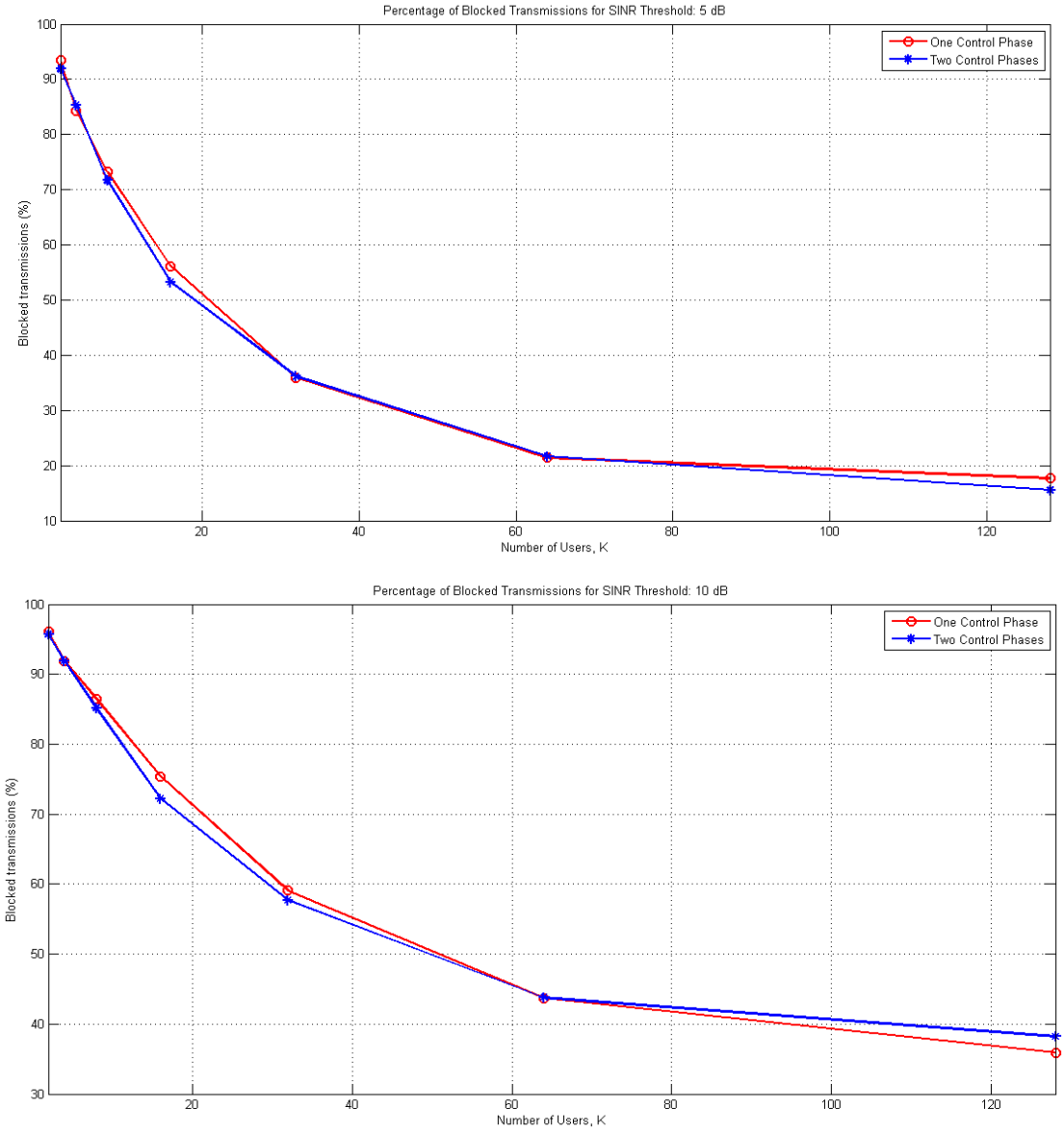

Fig. 14: Percentage of licensee system's blocked transmissions versus the number of mobile users *K* for transmit power over noise variance ratio *P* = 15 dB for both incumbent and licensee BS and different SINR thresholds.

5.4.3 Joint OBF with DC-MPFS and System Dimensioning

Next, we focus on a variation of the above setup where the normalized transmission power of the licensee BS (with respect to the noise power) is $P_2 = 5$ dB. We assume that the buffer for each user is expressed as an infinite length queue. The request process is described as a Poisson

process with mean arrival rate $\lambda = 1$. In this system we study the performance of joint OBF with PFS as well as with the new scheduler delay constraint maximum proportional fair scheduler (DC-MPFS), see [27]. In the latter algorithm the denominator in $R_k(t)/T_k(t)$ is not the average throughput over a sliding window of size W but it is the maximum throughput instead. Moreover, this fraction is scaled by the normalized delay, expressed as the mean delay encountered for the service of each user in this window over the maximum delay.

In Fig. 15 the average throughput of the system for SINR threshold $\gamma_{Th}^{\text{Inc}} = 0$ and 5 dB is shown, where it is observed that:

- As the number of users grows, the performance of the system improves due to the MU-Div effect.
- The average throughput benefits from a decrease of the QoS target (SINR threshold).
- The new scheduler outperforms PFS. The performance gap becomes more prominent for large user populations or / and as the SINR threshold increases.

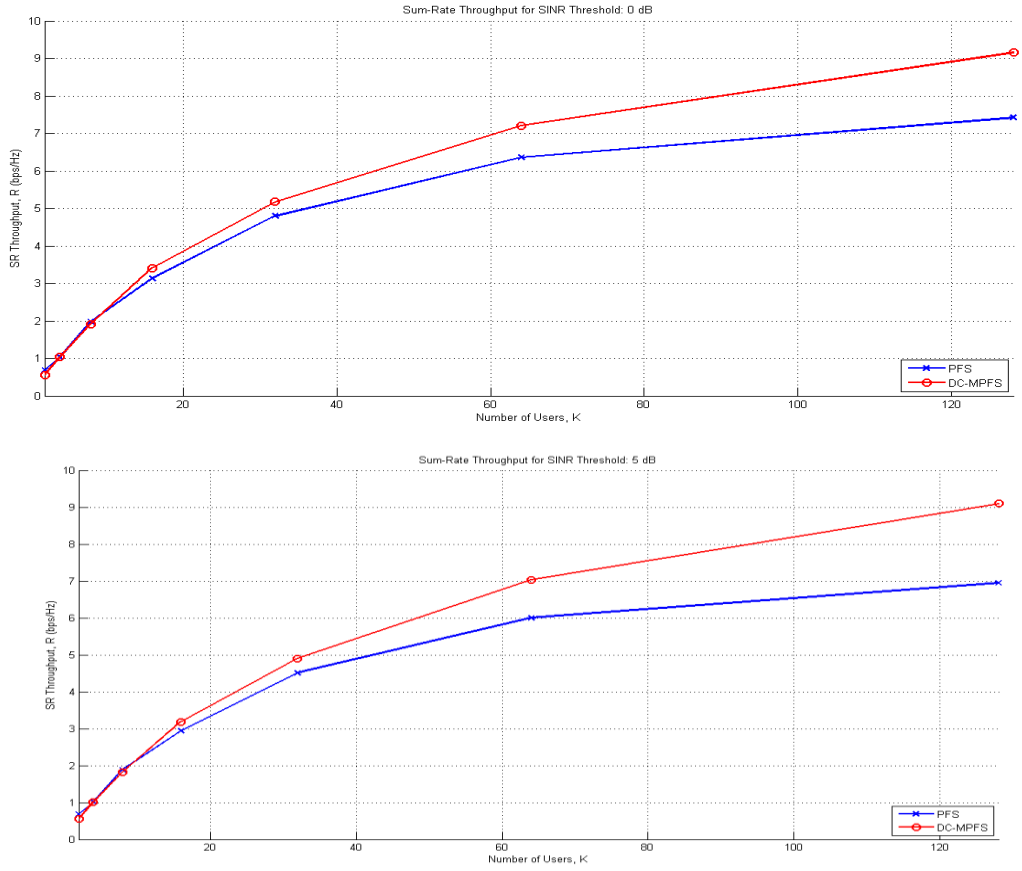

Fig. 15: Average system throughput versus the number of mobile users for various SINR thresholds.

In order to investigate on why DC-MPFS performs better than PFS, we have checked the percentage of the licensee system's blocked transmissions for a given SINR threshold $\gamma_{Th}^{\text{Inc}} = 0$

dB. As demonstrated in Fig. 16, the new scheduler results in less blocked transmissions than PFS, especially for large user populations.

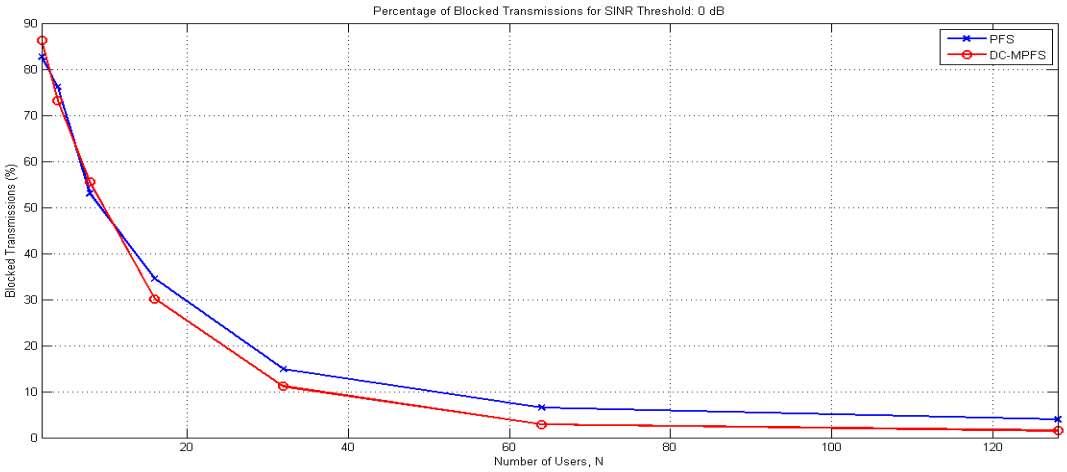

Fig. 16: Percentage of licensee's blocked transmission versus the number of mobile users for SINR threshold of 0 dB.

Finally, in Fig. 17, we show the breakdown of the individual data rates of the incumbent and the licensee system when PFS or DC-MPFS is utilized for $\gamma_{Th}^{\text{Inc}} = 0$ in comparison with the corresponding data rates achieved in the ideal scenario where the system under study is isolated (i.e., the other system is idle). We note that:

- In both variants, only a minor performance degradation is encountered by the incumbent's system. (In DC-MPFS, the performance gap between the use case where the licensee system becomes active or idle according to the established rules and the one where it is always is idle is negligible.)
- DC-MPFS achieves better data rate for both the incumbent and the licensee.

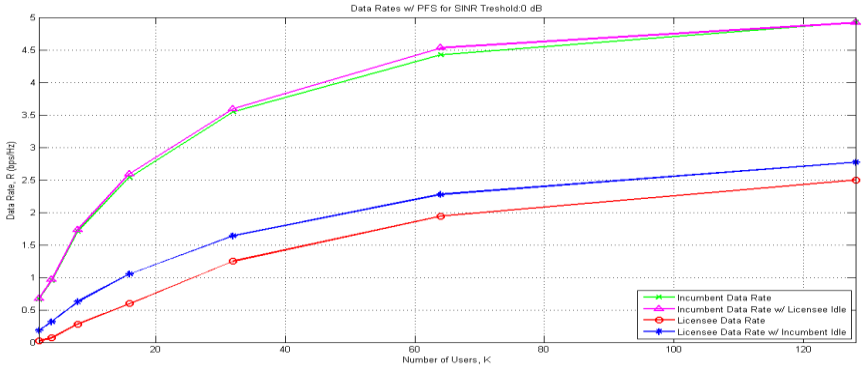

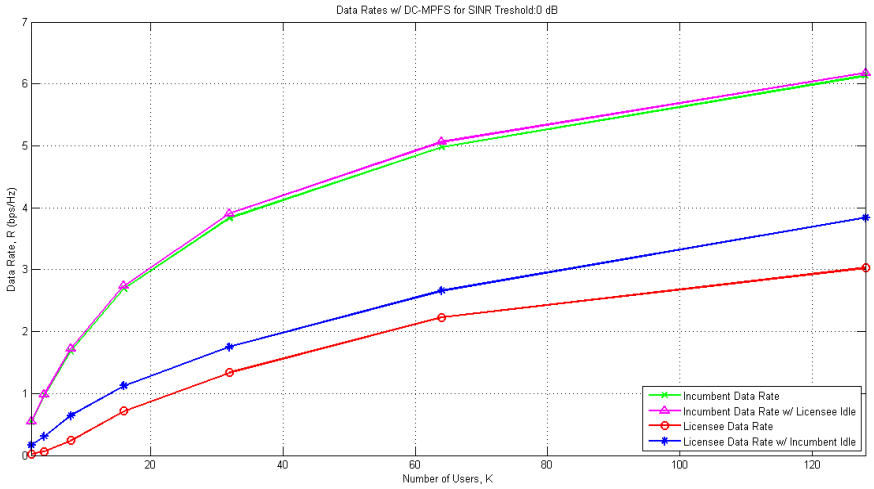

Fig. 17: Data rates versus the number of mobile users for SINR threshold of 0 dB.

5.4.4 Cooperative Opportunistic Transmission for Dynamic LSA

Next, we study a dynamic LSA system wherein three partially overlapping micro-cells belonging to the licensee are placed within a sector of a macro-cell belonging to the incumbent. The licensee is allowed to transmit simultaneously with the incumbent, provided that a predictable QoS level is ensured for the users of ***both*** systems. In order to accomplish this task as well as to limit the required communication/cooperation overhead, the small-cell BSs (SBS) make use of OBF with PFS and follow a simple cooperation approach. This consists of finding every time the optimum, in terms of the achieved sum-rate, *n*-tuple of small-cells ($n = 0, \dots, 3$) to transmit without causing intolerable interference to the users of the macro-cell BS or any of the small-cell BSs. The considered setup is illustrated in Fig. 18.

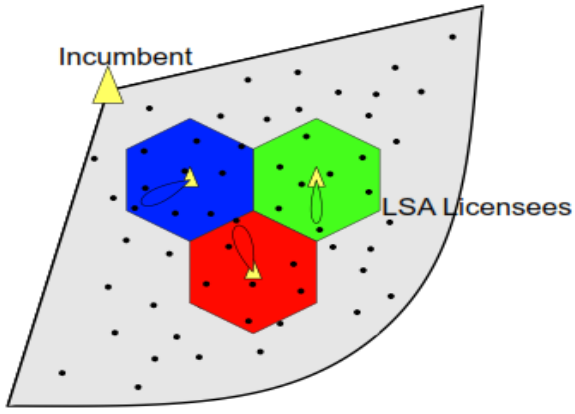

Fig. 18: System setup.

Scenarios and Cooperation Scheme

We consider two different scenarios. In the baseline scenario, the licensee's BSs transmit in a round-robin (RR) fashion. An SINR threshold is set for the incumbent user network and it is

considered to be available through the LSA repository. In any TS, the active SBS serves its preferred MU only if this potential transmission would not degrade the channel quality of the scheduled incumbent user below the predefined SINR threshold. Otherwise, the licensee BS remains idle in this TS. Note that in each TS the BSs choose a different random beam. Moreover, the users feed their instantaneous SINRs back to the serving BSs.

In the second scenario, which is closest to the LSA spirit, a SINR threshold is also set for the licensee's users. SBSs cooperate in order to provide the best possible performance for both the incumbent and the LSA licensee, under the QoS constraints, by deciding in a slot-by-slot basis which of them will transmit according to the coordination scheme described in Table .

Table 1: Cooperation between licensee's SBSs.

1. All SBSs transmit simultaneously, if no SINR threshold violations occur by these transmissions.
2. Otherwise, the best pair of SBSs, in terms of the achieved SR throughput, transmits, provided that the SINR threshold constraints are met.
3. Else, only one SBS from the previously selected pair transmits, given that it does not degrade the transmission of the incumbent below its predefined SINR threshold. The priority is given to the SBS with the highest rate.
4. If no combination / selection of SBSs can meet the given QoS requirements, then all of them remain idle and only the MBS serves its selected user, with the SNR-based rate this time, since there is no interference.

Signal Model

The baseband model that describes the incumbent and the licensee's received signal, with the application of the RR scheme, is expressed as:

$$y_k^{\text{Inc}}(t) = \underbrace{\sqrt{P_1}\mathbf{h}_{k,1}(t)\mathbf{x}_1(t)}_{\text{desired signal}} + \underbrace{\sqrt{P_l}\mathbf{h}_{k,l}(t)\mathbf{x}_l(t)}_{\substack{\text{interference} \\ (l=2,\ldots,4}} + \underbrace{n_k(t)}_{\text{noise}}, \quad (12)$$

$$y_{k,l}^{\text{Lic}}(t) = \underbrace{\sqrt{P_l}\mathbf{h}_{k,l}(t)\mathbf{x}_l(t)}_{\substack{\text{desired signal} \\ (l=2,\ldots,4}} + \underbrace{\sqrt{P_1}\mathbf{h}_{k,1}(t)\mathbf{x}_1(t)}_{\text{interference}} + \underbrace{n_k(t)}_{\text{noise}}, \quad (13)$$

where it is assumed that BS_1 refers to the MBS (incumbent), whereas BS_2 - BS_4 represent the SBSs (licensee). When the licensee remains idle, due to a SINR threshold violation, Eq. (12) reduces to Eq. (5). The corresponding SINRs are given by Eq. (3)-(4) and Eq. (6), respectively.

In the scenario where all SBSs transmit simultaneously, the baseband received signal at the scheduled user of the MBS is given by:

$$y_k^{\text{Inc}}(t) = \underbrace{\sqrt{P_1}\mathbf{h}_{k,1}(t)\mathbf{x}_1(t)}_{\text{desired signal}} + \underbrace{\sum_{l=2}^{4}\sqrt{P_l}\mathbf{h}_{k,l}(t)\mathbf{x}_l(t)}_{\text{interference}} + \underbrace{n_k(t)}_{\text{noise}}, \tag{14}$$

while the baseband received signal of the active user of BS_l $(l \neq 1)$ is

$$y_{k,l}^{\text{Lic}}(t) = \underbrace{\sqrt{P_l}\mathbf{h}_{k,l}(t)\mathbf{x}_l(t)}_{\substack{\text{desired signal}\\(l=2,\ldots,4)}} + \underbrace{\sum_{j \neq l}\sqrt{P_j}\mathbf{h}_{k,j}(t)\mathbf{x}_j(t)}_{\substack{\text{interference}\\(j=1,\ldots,4,\, j \neq l)}} + \underbrace{n_k(t)}_{\text{noise}}. \tag{15}$$

Similar relations also hold when two SBSs transmit. On the other hand, when only one SBS schedules a user or all SBSs remain idle, the corresponding equations collapse to ones of the RR scheme. The SINRs when all SBSs transmit simultaneously, are expressed as:

$$\gamma_k^{\text{Inc}}(t) = \frac{P_1\left\|\mathbf{h}_{k,1}(t)\right\|^2}{\sum_{l=2}^{4}P_l\left\|\mathbf{h}_{k,l}(t)\right\|^2 + \sigma_k^2} \tag{14}$$

$$\gamma_{k,l}^{\text{Lic}}(t) = \frac{P_l\left\|\mathbf{h}_{k,l}(t)\right\|^2}{\sum_{\substack{j=1\\ j\neq l}}^{4}P_j\left\|\mathbf{h}_{k,j}(t)\right\|^2 + \sigma_k^2}, \quad l = 2,\ldots,4. \tag{15}$$

5.4.5 Key Results

The proposed system has been evaluated in terms of the achieved average throughput at the incumbent and the licensee through numerical simulation results. The obtained throughput values are compared with the throughputs obtained for the incumbent (licensee) when the licensee (incumbent) is inactive, assuming that the rules defined in each scenario still hold for the SS.

Moreover, besides Scenario 1 (round robin) and 2 (cooperation), an upper bound for the performance of the system is used for comparison. More specifically, in the Scenario 3, the coexisting small cells are isolated from each other such that they form three orthogonal (i.e., non-interfering) (4,1) Multiple Input Single Output (MISO) channels with their selected users. The SBSs transmit simultaneously. Since we use the performance of this system as a benchmark, we do not consider any SINR thresholds that would lead to a decision-making process that might force the licensee to not allow all three SBSs transmit simultaneously. In the absence of the macro-cell interferer, it is well known that, due to its orthogonality, this setup is the optimum one when each BS schedules only a single user in each TS. With the incumbent present, it is still optimum because in the capacity regime all signals, including the one transmitted from the incumbent, are Gaussian. Thus, this setup is similar to the one with the incumbent absent (but with worse SINR due to the interference caused by the incumbent).

Performance results are obtained over 1000 simulation runs with an increasing total number of users (8, 16, 32, 64, 128); transmit powers P_1 = 15W for the macro-cell BS and P_l = 1W (l =

$2, \ldots, 4$) for the micro-cell BSs; PFS window size W = 100 TS; and SINR thresholds either 0dB or 1dB (i.e., four different incumbent-licensee SINR threshold combinations).

Note that the setting of the appropriate values for the SINR thresholds depends on multiple factors, such as the transmit power and noise power level, the geometry of the considered setup, the severity of fading etc. We have focused on the low SINR values regime, which not only suits the transmission profile of the considered system, but also reflects closer the reality. It should be noted that we have also considered in the simulation the path loss, shadowing and small-scale fading effects.

Fig. 19 shows the average throughputs of the incumbent and the licensee in the considered use cases versus the size of the user population for various combinations of corresponding SINR thresholds. This simple, minimal cooperation scheme lies between the two extreme cases of Round-Robin (Scenario 1) and Orthogonal (Scenario 3) setups in terms of average throughput (usually above the half-way point), while causing only a slight degradation to the performance of the incumbent. Moreover, this low-feedback cooperation technique performs better than the Round-Robin system even when the SBSs are isolated (i.e., the MBS is idle). Furthermore, it is apparent that this method exploits MU-Div. Finally, we observe that as the value of the SINR thresholds increases, the performance of the licensee in the relevant scenarios becomes worse, since then SINR threshold violations occur more often and, therefore, some SBS transmissions might be blocked.

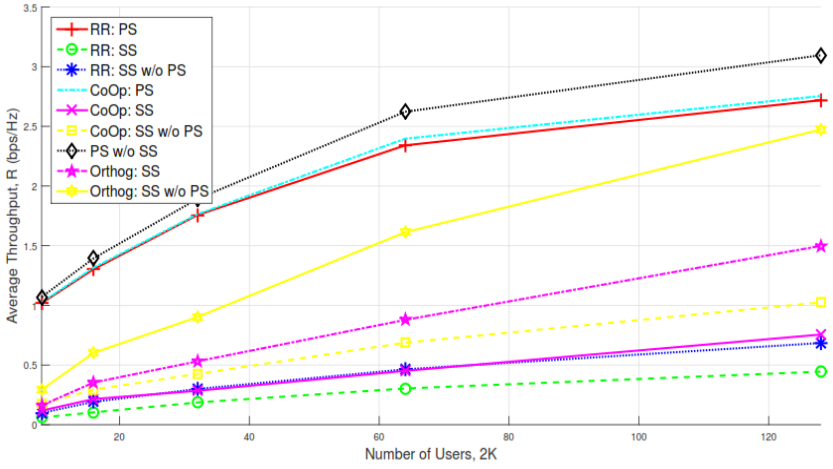

(a)

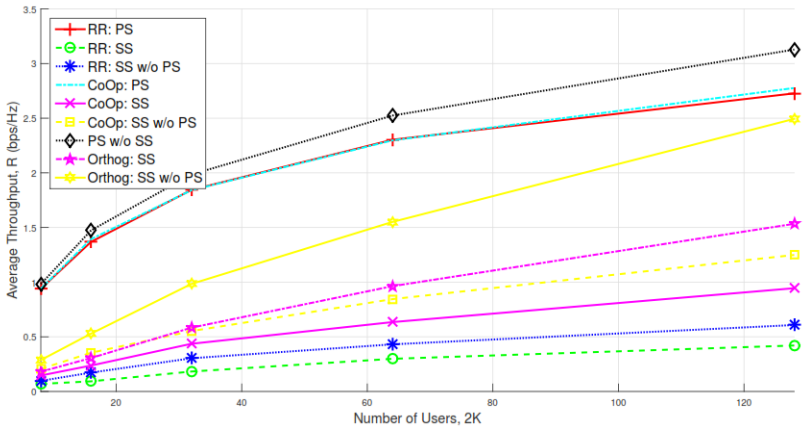

(b)

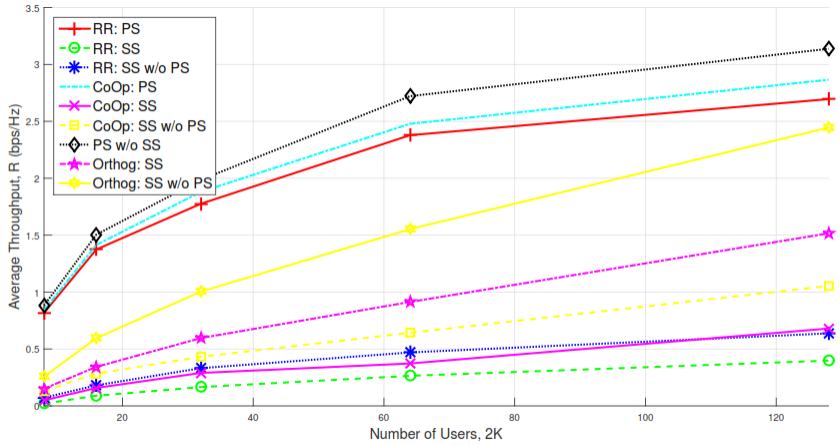

(c)

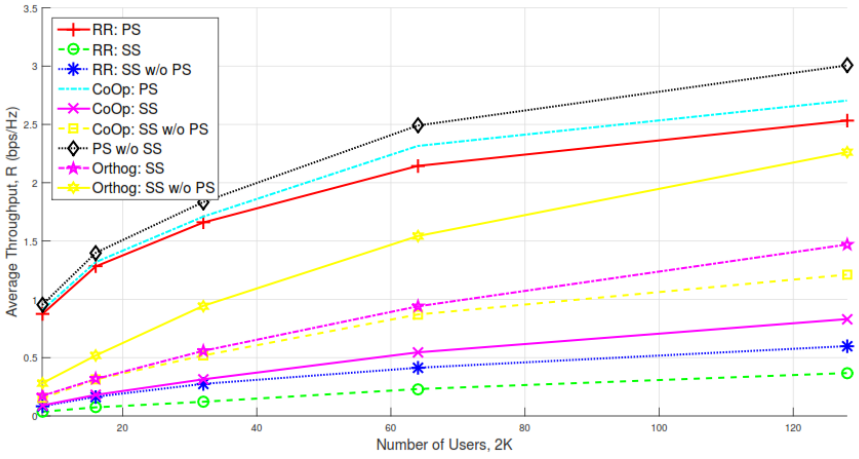

(d)

Fig. 19: Data rates of primary system (PS) and secondary system (SS) – i.e., incumbent and licensee – vs. the number of users for various use cases and for the SINR Threshold combinations (Incumbent, Licensee): (a) (0,0), (b) (0,1), (c) (1,0) and (d) (1,1) dB.

5.5 MIMO OFDM Capacity Maximizing Spatial Transceiver Design for the High Doppler Train Scenario

In the ADEL train scenario, LSA gets exploited to provide high data rate backhaul between the train and the fixed wireless infrastructure (this does not concern the data service for the small cell within the train). As the train (e.g. TGV) is moving fast, connectivity for the backhaul is short lived and hence needs to be exploited to the fullest with high data rate spatial multiplexing techniques (MIMO). On the other hand, the train moves on known tracks which leads to predictability of the slow fading aspects, allowing location aided anticipatory resource allocation [16]. On the other hand, also the fast fading can be managed to some extent via location aided Doppler compensation (receiver or transmitter based).
The multipath propagation and time varying Doppler shifts as shown in Fig.20 [10]. We consider an OFDM scenario and assume a linear model for the ICI caused by the Doppler. We then determine the optimal transmit precoders and the power allocation for each OFDM subcarrier that optimizes the sum capacity in such a scenario [11]. We extend this design by exploiting the excess cyclic prefix (ExCP) to further mitigate ICI in an OFDM system [12]. As the original cost function is non-convex, the beamformer design is done in an iterative manner. We first follow the difference of convex functions approach to obtain a convex cost function. However, we reinterpret this approach as a majorization technique. To solve the joint problem of power allocation across subcarriers and precoder design for all the useful subcarriers, we employ the cyclic minimization approach to alternately optimize the precoder design and transmit power allocation across subcarriers. The convergence of the iterative approach is proved and the theory is validated via numerical simulations.

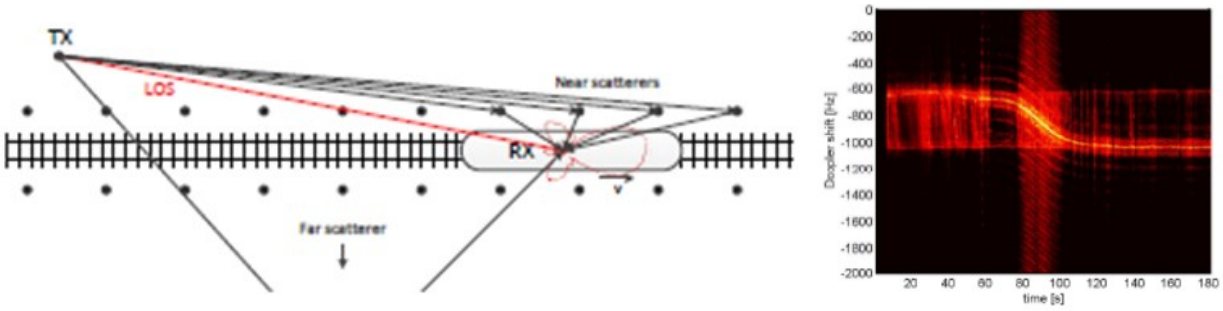

Fig. 20. Multipath propagation for the train backhaul (left) and pathwise time-varying Doppler shifts (right).

5.5.1 Problem formulation

Initial direction that we pursued involved a focus on a per path approach (esp. Line-of-Sight (LoS)). In this approach we perform location aided Doppler compensation of the path and zero-forcing (ZF) (beamforming (BF)) of the other paths. In Fig. 20 one observes indeed what appears to be an impressive Doppler variation for the LoS path. The Doppler shifts involved can be expected to lead to impressive InterCarrier Interference (ICI) in an OFDM transmission setting. This motivates the per path Doppler compensation approach. We formulated max SINR (I=ICI) joint BF and

Doppler compensation and we found e.g. that the optimal Doppler compensation is close to one obtained by (standard) Cyclic Prefix (CP) based Doppler compensation.
It turns out that eventually we realized that with the LTE OFDM structure, even TGV speed of 450kmph leads to limited channel variation. The channel variation is approximately linear over the duration of an OFDM symbol. This also means that the different multipath contributions cannot be differentiated over the duration of an OFDM symbol on the basis of their Doppler shift.
Fig. 21 analyzes the goodness of linear channel variation assumption for a typical LTE scenario with center frequency 2.4GHz and channel spacing 15KHz. Residual ICI beyond what is predicted by the linear model is given by the red curve. Approximation error due to linear modelling of ICI is negligible up to 450Kmph (Doppler frequency = 1 KHz) assuming operating SNR less than 35dB.

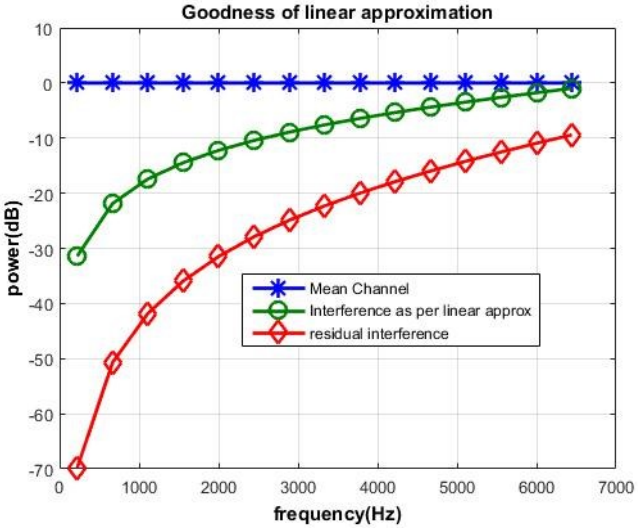

Fig. 21. Goodness of linear approximation for ICI as a function of Doppler frequency.

For every combination of Tx (transmit) and Rx (receive) antenna, the time domain channel at sample n of an OFDM symbol may be represented as

$$\mathbf{h}(n) = \mathbf{h}_0 + (n - \frac{N-1}{2})\mathbf{h}_1$$

where $\mathbf{h}_1$ is a constant across the OFDM symbol and captures the time variation per sample. $\mathbf{h}_0$ represents the mean channel across the OFDM symbol. Upon taking the N-point FFT, the frequency domain representation of carrier index k across the N_r receive antennas would become

$$\mathbf{y}_k = \mathbf{H}_{0k}\mathbf{d}_k + \sum_{l=0,l\neq k}^{N-1} \mathbf{H}_{1l}\mathbf{d}_l \Xi_{k,l} + \hat{\nu}_{\mathbf{k}}, \qquad \Xi_{k,l} = \frac{1}{N}\sum_{n=0}^{N-1}\left(n - \frac{N-1}{2}\right) e^{j2\pi(k-l)\frac{n}{N}}$$

$\mathbf{H}_{0k}$ is the mean frequency domain channel observed at subcarrier k. The second term in equation above represents the ICI (inter carrier interference) caused by time variance due to Doppler. $\mathbf{H}_{1k}$ is the frequency domain channel component corresponding to $\mathbf{h}_1$ at subcarrier k, $\mathbf{d}_k$ corresponds to vector of transmitted data symbols on the carrier k. Let the transmit covariance matrix of subcarrier k be $\mathbf{Q}_k = E(\mathbf{d}_k\mathbf{d}_k^H)$ where E(.) is the expectation operator. The objective in [11] to

determine the optimal $\mathbf{Q}_k$ for each subcarrier k such that the capacity of the link is maximized under a power constraint.

$$\mathtt{f}_0 : \max_{\mathbf{Q}_k} \sum_{k=0}^{N-1} \log \left|\mathbf{I}+\mathbf{H}_{0k}\mathbf{Q}_k\mathbf{H}_{0k}^H\bar{\mathbf{R}}_k^{-1}\right| \quad \mathtt{subject\ \ to} \quad \sum_{k=0}^{N-1} \mathtt{tr}\left\{\mathbf{Q}_k\right\} \leq P$$

Another important tool in the mitigation of ICI is the exploitation of excess CP (cyclic prefix). With an appropriate window function, the excess CP at the receiver may be exploited to reduce the ICI. This is particularly relevant for HST scenarios where due to the close proximity of the Base station towers to the railway tracks, the delay spread expected is very minimal. The significance of using the excess CP and the Nyquist criterion can be found in [13]. For a single input single output (SISO) scenario, optimal window coefficients were derived to minimize the combined ICI and noise power in [14]. More recently, a raised cosine window was used in [15] in an orthogonal frequency division multiple access (OFDMA) uplink scenario with varying carrier frequency offsets (CFO) across different users to reduce the extent of spread of ICI across the subcarriers. This was in turn utilized to aid in inverting an ICI interference matrix. In [12], the transmit beamformer design takes into account the excess CP exploitation at the receiver. In fact, we jointly optimize both the receive window and the transmit beamformer using a cyclic minimization approach.

5.5.2 Key results

The overall algorithm to determine the optimal beamformer may be summarized as follows

- Update the covariance matrix $\mathbf{Q}_k$ for every subcarrier k.

  The optimal beamforming directions $\mathbf{V}_i$ (containing unit norm columns) can be interpreted as solution for the generalized Eigen matrix condition.

  $$\mathbf{A}_i\mathbf{V}_i = \left(\mathbf{B}_i + \mu_i\mathbf{I}\right)\mathbf{V}_i\mathbf{\Sigma}$$

  where

  $$\mathrm{Q}_i = \mathbf{V}_i\mathbf{\Lambda}_i\mathbf{V}_i^H, \mathrm{A}_i = \mathbf{H}_{0i}^H\bar{\mathbf{R}}_i^{-1}\mathbf{H}_{0i} \text{ and } \mathbf{\Sigma} \text{ is a diagonal matrix}$$

  The power allocation across the antennas for subcarrier k is done using the ICI aware water filling method.

- Based on the transmit direction obtained from the above step, update the power across all carriers and all antennas using the ICI aware water filling method.

- Iterate the above two steps in alternating minimization till convergence.

The first step in the above algorithm is a step in majorization and is hence non-decreasing. The next step does alternating minimization and hence is also non-decreasing, thereby ensuring the non-decreasing behavior of the overall algorithm.

Fig. 22 gives the channel capacity convergence in the case of 6 Tx and 3 Rx antennas for the case of an OFDM system with 16 subcarriers. The non-decreasing behavior of the algorithm may be observed clearly. In the absence of ICI, Fig. 23 shows that the performance of the algorithm is the same as that of the standard OFDM waterfilling algorithm. In Fig. 24, as there is an excess of receive antennas, the ICI cancellation from the transmit antennas give only marginal performance improvement.

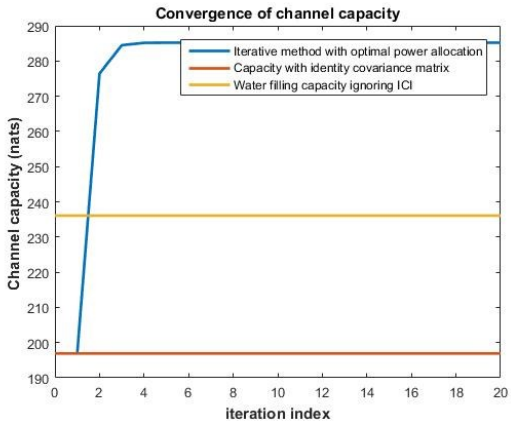

Fig. 22. Channel capacity convergence for 6 Tx, 3 Rx scenario, 1KHz Doppler.

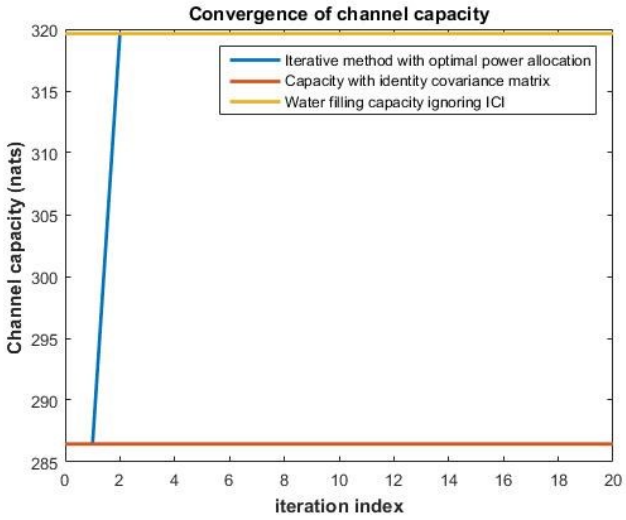

Fig. 23. Channel capacity convergence for 6 Tx, 3 Rx scenario, No Doppler.

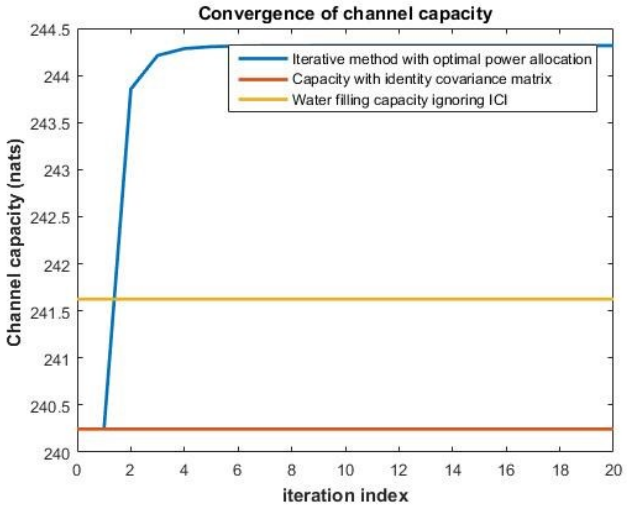

Fig. 24. Channel capacity convergence for 3 Tx, 5 Rx scenario, 1kHz Doppler.

Fig 25 shows the channel capacity convergence with window parameter optimization for the excess CP where an OFDM system with 16 subcarriers and excess cyclic prefix length of 8 is considered. Performance if compared with and without exploitation of excess CP. Further, the optimized window coefficients are compared against the root cosine window coefficients. Fig 26 further compares the roll off in frequency domain for the optimized window against other windows. It can be clearly seen that the optimal window is able strike a good balance between the attenuation of the adjacent side lobes and the side lobes farther away.

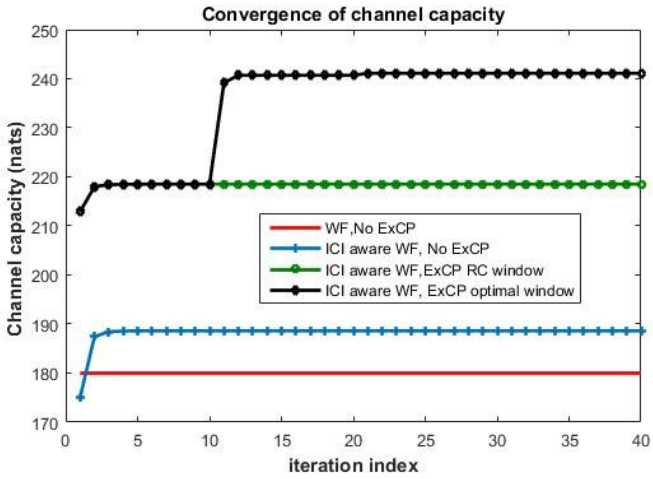

Fig. 25. Channel capacity convergence with excess CP exploitation for 3 Tx, 3 Rx scenario, 1kHz Doppler

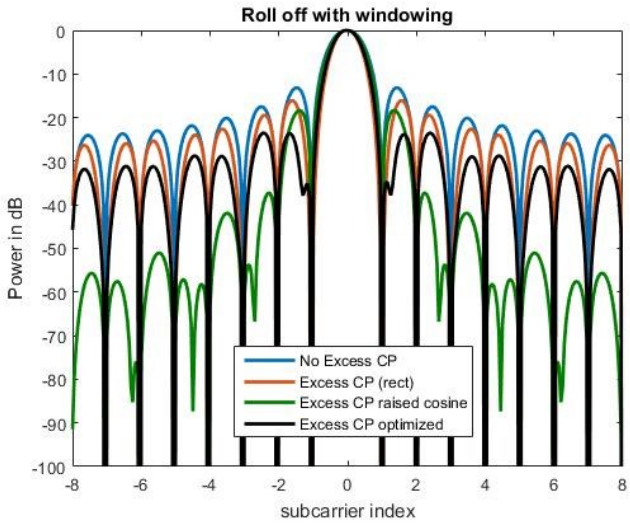

Fig. 26. Roll off in the frequency domain for different window functions, 3 Tx 3 Rx, 1KHz Doppler

5.5.3 Future work

In our future work, we shall explore the design of the MIMO transmit beamformer under partial CSIT instead of the full CSIT that is being assumed currently. Indeed, in the situation considered in which the channel is varying fast, even within an OFDM symbol, the availability of accurate CSIT is quite problematic. In practice, regardless of whether channel feedback is used in FDD or channel reciprocity is exploited in TDD, there will be significant delay between the last time instant at which the channel is estimated and the time it gets exploited in the OFDM symbol considered. Hence channel prediction needs to be performed, leading to channel prediction error among other forms of channel error in the partial CSIT.

5.6 From Multi-Antenna Underlay to LSA Coordinated Beamforming

We consider exploiting multiple antennas for a much more dynamic form of Licensed Shared Access (LSA) in the form of Coordinated Beamforming (CoBF) between incumbent cells and licensee cells. The BF is based on a combined form of partial CSIT (Channel State Information at the Transmitter(s) (Tx)), comprising both channel estimates (mean CSIT) and covariance CSIT. In particular multipath induced structured low rank covariances are considered that arise in Massive MIMO (MaMIMO) and mmWave settings. For the beamforming optimization, we first revisit Weighted Sum Rate (WSR) maximization with perfect CSIT. We then turn to the partial CSIT case where we consider Expected WSR (EWSR) maximization for which the MaMIMO limit turns out to be a (much) better approximation compared to the existing Expected Weighted Sum MSE (EWSMSE) approach. We then show how WSR maximization in CoBF leads to optimized values for the Lagrange multipliers that appear in BF for underlay cognitive radio with interference

temperature constraints. The work considered here is applicable to both macrocellular or small cell or even heterogeneous scenarios.

5.6.1 Problem formulation

In this section, Tx may denote transmit/transmitter/transmission and Rx may denote receive/receiver/reception. Interference is the main limiting factor in wireless transmission. Base stations (BSs) disposing of multiple antennas are able to serve multiple Mobile Terminals (MTs) simultaneously, which is called Spatial Division Multiple Access (SDMA) or Multi-User (MU) MIMO. However, MU systems have precise requirements for Channel State Information at the Tx (CSIT) which is more difficult to acquire than CSI at the Rx (CSIR). Hence we focus here on the more challenging downlink (DL). The main difficulty in realizing linear IA for MIMO I(B)C is that the design of any BS Tx filter depends on all Rx filters whereas in turn each Rx filter depends on all Tx filters [17]. As a result, all Tx/Rx filters are globally coupled and their design requires global CSIT. To carry out this Tx/Rx design in a distributed fashion, global CSIT is required at all BS [18]. The overhead required for this global distributed CSIT is substantial, even if done optimally, leading to substantially reduced Net Degrees of Freedom (DoF) [19]. The recent development of Massive MIMO (MaMIMO) [20] opens new possibilities for increased system capacity while at the same time simplifying system design. We refer to [21] for a further discussion of the state of the art, in which MIMO IA requires global MIMO channel CSIT. Recent works focus on intercell exchange of only scalar quantities, at fast fading rate, as also on two-stage approaches in which the intercell interference gets zero-forced (ZF). Also, massive MIMO in most works refers actually to MU MISO.

Whereas the exploitation of covariance CSIT may be beneficial, in a MaMIMO context it may quickly lead to high computational complexity and estimation accuracy issues. Computational complexity may be reduced (and the benefit of covariance CSIT enhanced) in the case of low rank or related covariance structure, but the use and tracking of subspaces may still be cumbersome. In the pathwise approach, these subspaces are very parsimoniously parameterized. In a FDD setting, these parameters may even be estimated from the uplink (UL). In a TDD setting with reciprocity, the channel estimation error may account for time variation also in the UL/DL ping-pong. As opposed to the instantaneous channel CSIT, the path CSIT is not affected by fast fading. Whereas path CSIT by itself may allow zero forcing (ZF) [22], which is of interest at high SNR, we are particularly concerned here with maximum Weighted Sum Rate (WSR) designs accounting for finite SNR. ZF of all interfering links leads to significant reduction of useful signal strength. Massive MIMO makes the pathwise approach viable: the (cross-link) beamformers (BF) can be updated at a reduced (slow fading) rate, parsimonious channel representation facilitates not only uplink but especially downlink channel estimation, the crosslink BF can be used to significantly improve the downlink direct link channel estimates (in FDD), minimal feedback can be introduced to perform meaningful WSR optimization at a finite SNR (whereas ZF requires much less coordination).
In [24] we first review some recent approaches for maximizing WSR, based on a link to Weighted Sum MSE (WSMSE) and an approach based on Difference of Convex function programming (which is actually better interpreted as an instance of majorization). We then consider various approaches for maximizing Expected WSR (EWSR) for the case of partial CSIT. The existing EWSMSE approach [25] improves over Naive EWSR (NEWSR) by accounting for covariance

CSIT in the interference. This can have significant impact, even on the sumrate prelog (DoF) if the instantaneous channel CSIT quality does not scale with SNR. A further improvement is proposed here in the ESIC-WSR (Expected Signal and Interference Covariance) approach which represents a better approximation of the EWSR. In a MaMIMO setting, the way mean and covariance CSIT are combined in the EWSMSE or ESIC-WSR approaches for the interference terms becomes equally optimal as in the EWSR for a large number of users. ESIC-WSR represents an improvement over EWSMSE for capturing the signal power (matched filtering and diversity aspects) and only leads to a finite (dB) gain (in SNR), but its remaining approximation error over EWSR may be limited. Strictly speaking, in the large number of users setting, EWSMSE ≤ EWSR ≤ ESIC-WSR. The step from EWSMSE to ESIC-WSR also deals with the following question. Covariance CSIT can be used to improve the channel estimate from a basic deterministic estimate to a Bayesian estimate. The question then arises: is that enough? The answer is no and a first take at this issue is proposed here. This work is a followup on [23] from which we reproduce some sections to ease reading. In [23], we introduced a heuristic to design the Tx separately using path CSIT only. It turns out that this heuristic is recovered by the ESIC-WSR approach proposed here, which furthermore provides expressions for a number of auxiliary quantities that are needed and allows the combination of channel estimate and path CSIT.
The combined exploitation of channel estimate CSIT and channel covariance CSIT (inherited from a pathwise propagation channel structure) can be done by formulating a Gaussian channel distribution. However, it is pointed out in [24] that a deterministic channel estimate plus prior covariance information should first be transformed to a posterior Gaussian distribution, centered at the posterior mean, with a posterior covariance, before exploiting it in a EWSR expression. Also, in the MaMIMO limit, in fact only the first two channel moments count and the Gaussian distribution assumption is unimportant.
In this work we consider multiple cells (incumbent and licensee) with multi-antenna BS serving possibly multiple users with single or multiple antennas.

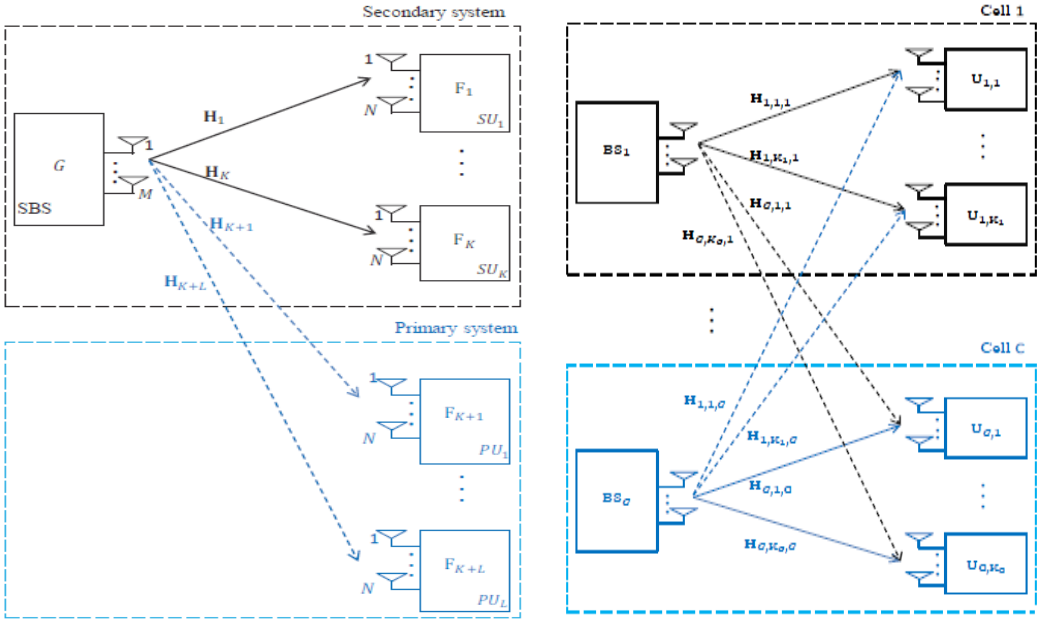

Fig. 27. Traditional underlay cognitive radio systems (left) vs. coordinated beamforming in multiple cells (right).

5.6.2 Key results

We first have introduced an iterative beamformer design algorithm for maximum weighted sum rate (WSR). The KKT conditions for the BF lead fairly straightforwardly to the optimal BF being a maximum generalized eigenvector of the form

$$\mathbf{g}_k' = V_{max}(\mathbf{H}_k^H \widehat{R}_k^{-1} \mathbf{H}_k, \sum_{i=1,\neq k}^{K} u_i \mathbf{H}_i^H (\widehat{R}_{\bar{i}}^{-1} - \widehat{R}_i^{-1}) \mathbf{H}_i + \lambda I)$$

In fact, these BF turn out to be optimized forms of heuristic solutions that have been introduced to maximize a so-called Signal-to-Leakage-plus-Noise-Ratio (SLNR), in which the Leakage represents the Interference caused to other users when transmitting, similar to the familiar Signal-to-Interference-plus-Noise-Ratio (SINR) at a receiver:

$$SLNR_k = \frac{||\mathbf{H}_k \mathbf{g}_k||^2}{\sum_{i \neq k} ||\mathbf{H}_i \mathbf{g}_k||^2 + \sum_i ||\mathbf{g}_i||^2 / P} \text{ vs}$$

$$SINR_k = \frac{||\mathbf{H}_k \mathbf{g}_k||^2}{\sum_{i \neq k} ||\mathbf{H}_k \mathbf{g}_i||^2 + \sum_i ||\mathbf{g}_i||^2 / P} .$$

The SLNR optimizing BF is also a generalized eigenvector, but of unweighted quantities:

$$\mathbf{g}_k' = V_{max}(\mathbf{H}_k^H \mathbf{H}_k, \sum_{i \neq k} \mathbf{H}_i^H \mathbf{H}_i + I) .$$

The minorization of the WSR cost function by a concave approximation also leads to an optimization of the stream powers, in a fashion that can be interpreted as “interference aware water filling”. We then extended the perfect CSIT approach to optimization of the Expected WSR combining both channel estimates and covariance CSIT. The goal here is multifold. A naive approach would just perform (possibly Regularized) Zero-Forcing (R-ZF) BF. We derived algorithms that maximize the WSR at any finite SNR, exploiting not only channel estimate information, accounting for the channel estimation error level, but also exploiting channel covariance information. The resulting approach even works when only channel covariance information is available (e.g. for the intercell channels). This could arise when the user location information is translated into a channel covariance based on Line-of-Sight (LoS) propagation.

In the simulations below, we consider just a single cell MIMO system with 2 users, with CSIT based on the MIMO Ricean channel model (hence the CSIT comprises the (downlink) Tx side LoS antenna array response and the Rice factor μ both of which can be estimated from the uplink channel). In the figure the expected sum rate (SR) is plotted versus SNR for 4 Tx and Rx antennas and 2 users. For the Tx design, we consider either zero forcing (ZF) on the LoS component, with uniform power loading, or an optimized design based on the Massive MIMO limit for the DC program. For each design, three cases of Rice factor are considered: μ = 10; 100; ∞ (this last case is labeled ”Perfect CSIT” in Fig. 28). The expected SR is obtained by averaging over channel realizations, according to the Ricean distribution with respectively one of the three possible values

for μ. The optimized approach which accounts for CSIT imperfections and finite SNR clearly improves over naive (LoS based) ZF.

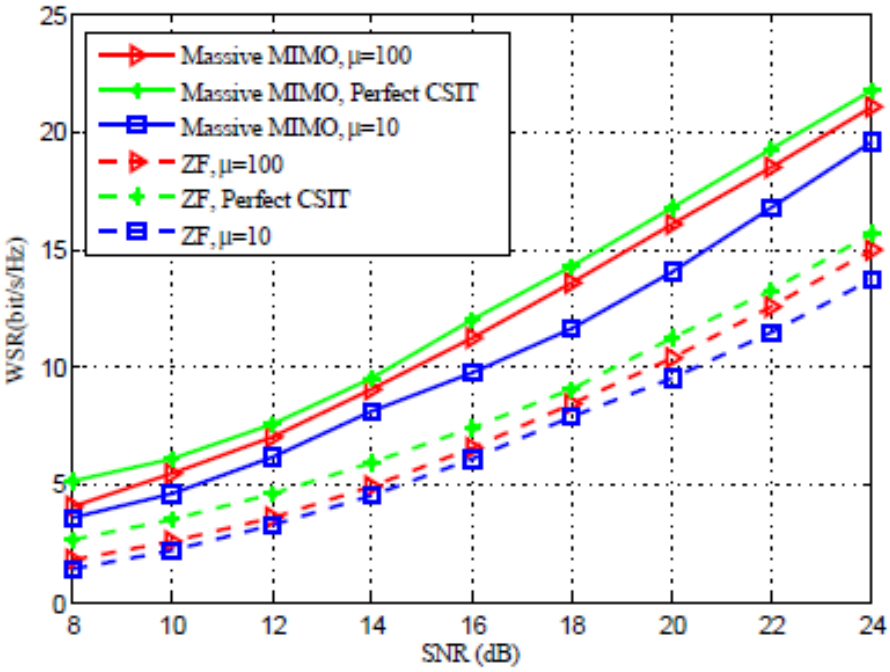

Fig. 28. EWSR vs SNR for 4 Tx and Rx antennas and 2 users.

We also establish an explicit link between underlay cognitive radio and coordinated beamforming: the optimal choice for the Lagrange multipliers for the interference temperature constraints in underlay cognitive radio in fact corresponds to the ratio of the rate weight (in the WSR) for the stream interfered with over the MSE attained for that stream.

5.6.3 Future work

In our future work, we shall focus on how to minimize the crucial information exchange between cells to realize CoBF. Also, the acquisition of covariance information, though very helpful, is a non-trivial issue, especially in MaMIMO. Exploiting the pathwise model is probably one of the more realistic approaches (more generally: low rank models), which then introduces also the issue of error on the covariance information.

5.7 Full-duplex spectrum sensing system

Within this task, we develop the full-duplex spectrum sensing system to realize the simultaneous spectrum sensing and secondary transmission. i) Firstly, the generalized expressions of the key sensing performance metrics are derived for multiple sensing antennas. Listen-and-talk protocol is applied and multiple sensing/transmission antennas are considered in this part. ii) Secondly, the optimal decision threshold pair is investigated in order to minimize the total error rate of the

system. Therefore, the benefits of primary and secondary users can be considered at the same time.

5.7.1 Problem Formulation

Full-duplex (FD) systems can conduct transmission and reception simultaneously at the same frequency bands, but self-interference will be introduced by the FD antennas. However, due to the recent advances on self-interference reduction techniques, the FD technique has been put forward to apply in cognitive radio (CR) networks to improve the sensing performance and spectral efficiency of the secondary network. In FD CR networks, the secondary user (SU) possesses FD capability and the antennas of the SU is partitioned into two parts, including the sensing and transmission antennas. Compared with the half-duplex (HD) CR network within the same length of periodic spectrum sensing frame, FD CR systems can implement sensing and transmission during the whole frame so that more samples can be accumulated for spectrum sensing and longer data transmission time can be obtained for the secondary network.

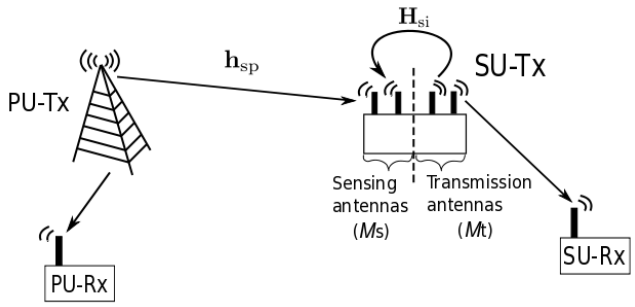

Fig. 29. The system model of the FD spectrum sensing

In practical CR systems, the realization of the synchronization between the primary and secondary networks is difficult since the types of these two networks are different normally. Therefore, the non-time-slotted model is considered in our work. Specifically, the system model of the FD spectrum sensing and non-time-slotted traffic are shown in Fig.29 and Fig. 30.

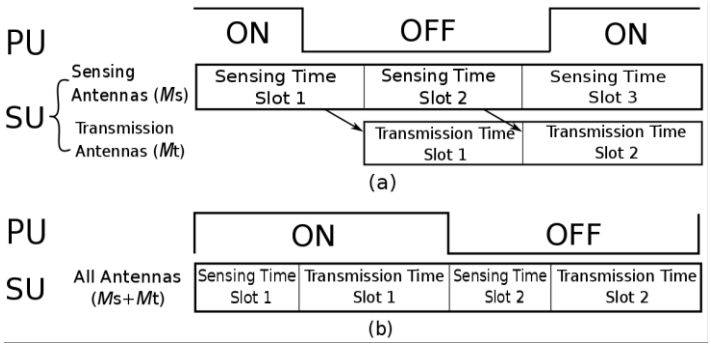

Fig. 30. (a) The FD non-time-slotted spectrum sensing system. (b) The HD time-slotted spectrum sensing system. (ON: The PU is active, OFF: The PU is inactive.)

5.7.2 Key results

The Sensing Performance of the FD Non-time-slotted System

In order to investigate the FD spectrum sensing system further in terms of optimal decision threshold and secondary transmission capacity, the generalized expression of the false alarm and detection rates are required for the general case of energy detector (ED) with multiple sensing antennas. It should be noted that the self-interference caused by the FD capability cannot be fully canceled. Therefore, the further research on the FD spectrum sensing system is conducted under the residual self-interference (RSI) in our work. In the non-time-slotted FD spectrum sensing system, the state of the PU is defined as the state at the end of each periodic frame of the SU's activity. Therefore, there exists 4 different hypotheses in terms of the activities of the PU and SU, which can be summarized as follows: (i) H_{10}: The SU is active (1), the PU is active for *a* samples and then turns to inactive (0) within the secondary periodic frame, (ii) H_{00}: The SU is inactive (0), the PU is active for *a* samples and then turns to inactive (0) within the secondary periodic frame, (iii) H_{11}: The SU is active (1), the PU is inactive for *b* samples and then turns to active (1) within the secondary periodic frame, (iv) H_{01}: The SU is inactive (0), the PU is inactive for *b* samples and then turns to active (1) within the secondary periodic frame, where $0 \leq a, b < N$ and *a, b* vary depending on the realistic situations, thus different cases are shown in simulation results for various *a, b*.

Different decision thresholds are required for the absence and presence of the secondary transmission due to the influence of the RSI. The expressions of the false alarm and missed detection rates under different scenarios are verified by simulations in Fig. 31. Meanwhile, the false alarm and missed detection rates of the system are shown by the receiver operating characteristic (ROC) curves in Fig. 32 and the comparison between the FD spectrum sensing and half-duplex (HD) is also revealed in this figure. From this figure, it can be deduced that the sensing performance of the whole system will degrade with the increase of the summation of *a* and *b*.

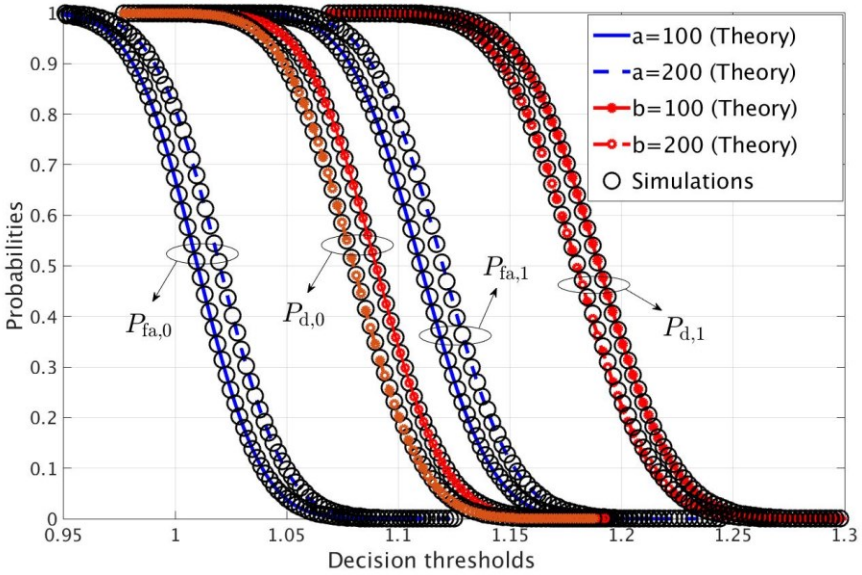

Fig. 31. The sensing performances under the hypotheses H_{11}, H_{10}, H_{01} and H_{00}.

Besides, when $a + b$ is constant, the sensing performance of the FD non-time-slotted CR system is similar no matter what the specific values of a and b are. In addition, it can be seen from the comparison with the HD spectrum sensing approach that the FD can achieve a better sensing performance based on the multi-sensing-antenna ED in the non-time-slotted CR network, since more received signal samples can be accumulated by employing FD technique.

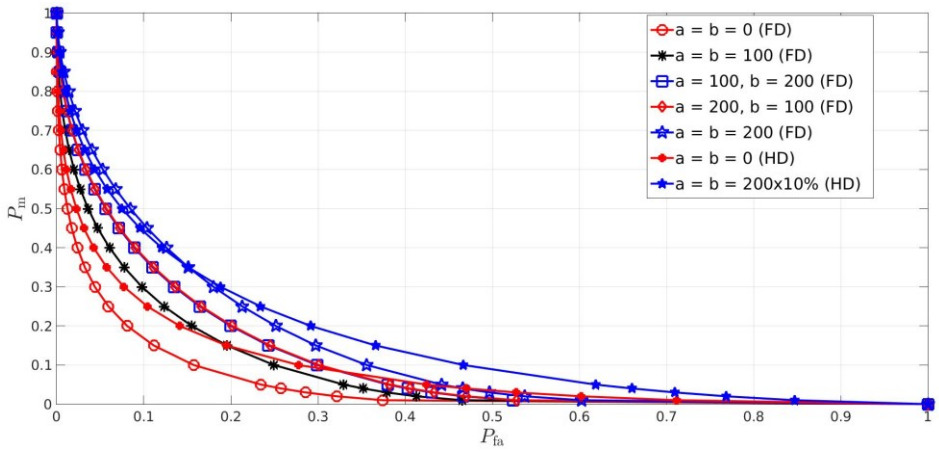

Fig. 32. The ROC curves of the FD spectrum sensing system and the comparison with the HD system.

Optimal Decision Threshold Pairs and Total Error Rates

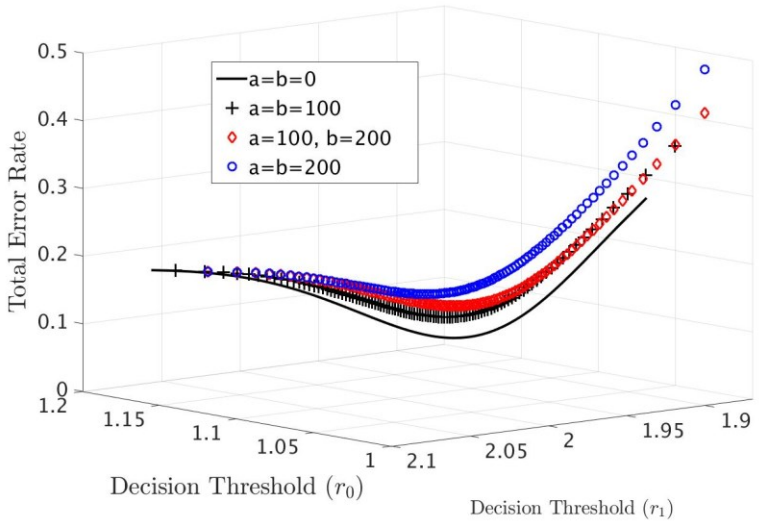

Fig. 33. The total error rate of the system V.S. the decision threshold pair (*r*0, *r*1)

In order to consider the benefits of the PU and SUs concurrently, the total error rate of the system is investigated and the optimal decision threshold pairs are obtained based on a given missed detection probability. The total error rate of the system is presented in Fig. 33 versus the different decision threshold pairs under different system conditions. The total error rate of the system

increases with the increasing $a + b$, since more signal samples with negative effects are received for spectrum sensing. Meanwhile, it can be also seen from this figure that the total error rate of the system is a quasi-convex function with regard to the decision threshold pairs. This implies that there exists one and only one optimal decision threshold pair to minimize the total error rate. Therefore, the optimal decision threshold pair can be obtained by using the derived equations in the last section. Specifically, the optimal decision threshold pairs $(\gamma_0, \gamma_1)_{opt}$ are (1.086, 1.974), (1.084, 1.980), (1.080, 1.980) and (1.085, 1.990) for the cases of ($a = b = 0$), ($a = b = 100$), ($a = 100$, $b = 200$) and ($a = b = 200$), respectively.

5.7.3 Future Work

(a) The sensing-based FD spectrum sharing model will be developed and the sensing performance will be studied. Specifically, the closed-form expressions of false alarm and missed detection rates will be derived and the method of determining the decision threshold for non-time-slotted system will be also discussed.

(b) Based on the sensing-based FD spectrum sensing, the throughput of the secondary network will be investigated and the optimal beamforming vector will be studied in order to maximize the secondary throughput.

5.8 Spectral Coexistence of Colocated MIMO Radars and Wireless Communications Systems

In this section, we consider the problem of effective spectrum sharing between a collocated Multiple-Input-Multiple-Output (MIMO) radar that monitors the existence of a target and a wireless communications system. The investigated scenario considers the downlink of a communications system represented by a Base Station (BS) trying to reuse the spectrum allocated for a colocated MIMO radar in order to communicate with an assigned terminal, in the vicinity of the radar system. We present an accurate model for the operation of the wireless system in the downlink, while the MIMO radar tries to maintain an acceptable detectability level of a target in the far field. The target detection problem is reformulated using a sensing approach based on energy detection, while the BS applies beamforming to null the interference created at the radar receiver. Based on the theory of Hermitian quadratic forms and with the aid of the Linearly Constrained Minimum Variance (LCMV) beamforming solution, the performance of target detection, when the MIMO radar coexists with the data transmission is quantified and numerical results show that spectral coexistence is feasible.

5.8.1 Problem Formulation

Let us consider the scenario of spectrum sharing between a colocated MIMO radar and an LTE wireless communications system. The communications system is assumed to consist of a base station (BS) that is equipped with M_1 transmit antennas, and the user equipment (UE) has a single antenna. The considered colocated MIMO radar is equipped with M_T transmitting antennas and MR receiving antennas. The interelement antenna spacing is denoted by d_r and measured in

wavelengths. The spacing between the radar elements is assumed identical for both transmitting and receiving elements. Following the common assumption in MIMO radar systems, the *target* is assumed a point-source at the far field. Considering the link between the radar and the target, let θ_{tar} be the direction of the target, and let θ_{BS} be the direction of the BS towards the radar. Furthermore, the environment is assumed clutter-free, and the point source is assumed stationary during the observation time.

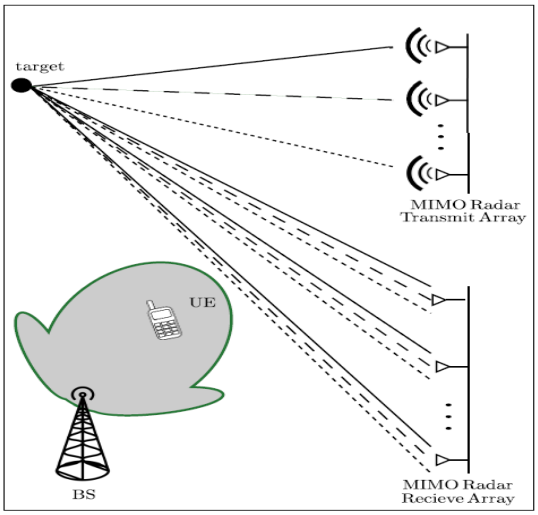

Fig. 34: Spectrum sharing scenario

The waveform vector, which is transmitted by the MIMO radar is

$$\boldsymbol{\phi}(t,\tau) \triangleq \left[\phi_1(t,\tau),\ldots,\phi_{M_{\mathrm{T}}}(t,\tau)\right]^{\top}$$

The transmit beamforming vector at the BS, is defined as

$$\boldsymbol{w}_1 = \begin{bmatrix} w_1 & w_2 & \ldots & w_{M_1} \end{bmatrix}^{\top}$$

Linearly Constrained Minimum Variance beamforming problem can be written as

$$\begin{aligned} \min_{\boldsymbol{w}} \quad & \boldsymbol{w}^{\mathrm{H}}\boldsymbol{R}_{ss}\boldsymbol{w} \\ \text{s.t.} \quad & \boldsymbol{C}^{\mathrm{H}}\boldsymbol{w} = \boldsymbol{f} \end{aligned}$$

where R_{ss} denotes the covariance matrix of the MIMO channel between the BS and the receive antennas of the radar, C is the constraint matrix and f is the response vector.

Let y_R denote the instantaneous signal received by the MIMO radar receive array.

$$\boldsymbol{y}_{\mathrm{R}}(t,\tau) = \begin{cases} \beta(\tau)\,\boldsymbol{a}_{\mathrm{R}}(\theta_{\mathrm{BS}})\,\boldsymbol{b}^{\top}\boldsymbol{w}_1 s_1(t,\tau) + \boldsymbol{z}(t,\tau), & \mathcal{H}_0 \\ \alpha(\tau)\boldsymbol{a}_{\mathrm{R}}(\theta_{\mathrm{tar}})\,\boldsymbol{a}_{\mathrm{T}}^{\top}(\theta_{\mathrm{tar}})\,\boldsymbol{\phi}(t,\tau) + \beta(\tau)\,\boldsymbol{a}_{\mathrm{R}}(\theta_{\mathrm{BS}})\,\boldsymbol{b}^{\top}\boldsymbol{w}_1 s_1(t,\tau) + \boldsymbol{z}(t,\tau), & \mathcal{H}_1 \end{cases}$$

Since the MIMO radar applies a target detection algorithm, based on energy detection, the decision statistic, will be of the following form:

$$\frac{1}{M_{\mathrm{R}}\, T_{\mathrm{rad}}} \|\widetilde{\boldsymbol{y}}(\tau)\|^2 \underset{\mathcal{H}_0}{\overset{\mathcal{H}_1}{\gtrless}} \eta,$$

where η is a predefined threshold chosen to achieve a specific pair of probability of false alarm and probability of missed detection.

The probability of false alarm and probability of detection are obtained as given by

$$\mathcal{P}_{\mathrm{fa}}(\eta) = \begin{cases} \sum_{i=1}^{M_{\mathrm{R}} T_{\mathrm{rad}}} \left(\prod_{q=1, q\neq i}^{M_{\mathrm{R}} T_{\mathrm{rad}}} \frac{\xi_q}{\xi_q - \xi_i} \right) \exp\left(-\xi_i \eta\right) & , \eta > 0, \\ 0 & \text{otherwise}, \end{cases}$$

$$\mathcal{P}_{\mathrm{d}}(\eta) = \begin{cases} \frac{1}{\Gamma(\hat{\delta})} \Gamma\left(\frac{1}{2}\hat{\delta}\,,\, \frac{\hat{\sigma}}{2}\left(\frac{\eta - \breve{\kappa}_1}{\sqrt{2\breve{\kappa}_2}} \right) + \frac{\hat{\mu}}{2} \right), & s_1^2 \leq s_2 \\ Q_{\frac{\hat{\delta}}{2}}\left(\sqrt{\hat{\delta}}, \sqrt{\hat{\mu} + \hat{\sigma}\left(\frac{\eta - \breve{\kappa}_1}{\sqrt{2\breve{\kappa}_2}} \right)} \right), & s_1^2 > s_2, \end{cases}$$

where $\Gamma(s, x) = \int_x^\infty t^{s-1}\, e^{-t}\, \mathrm{d}t$ is the upper incomplete gamma function, and $Q_k(a, b)$ is the k-th order Marcum Q-function

5.8.2 Key Results

Fig. 35 illustrates the BS array response when the BS applies LCMV beamforming to null its interference towards the MIMO radar. The results shown in the figure are obtained assuming a UE at direction 20 degrees, and the MIMO radar is at 80 degrees. The figure depicts the array response for two cases. The first case is when the MIMO radar is occupied with 4 transmit and receive antennas, and the second case is 8 antennas. The results in Fig.35 (a) implies the possibility of feasible coexistence. On the other hand, the results in Fig. 35 (b) implies that coexistence is not possible in this case, because the high level of interference caused by the BS will produce a significant deviation in the probabilities of false alarm and missed detection.

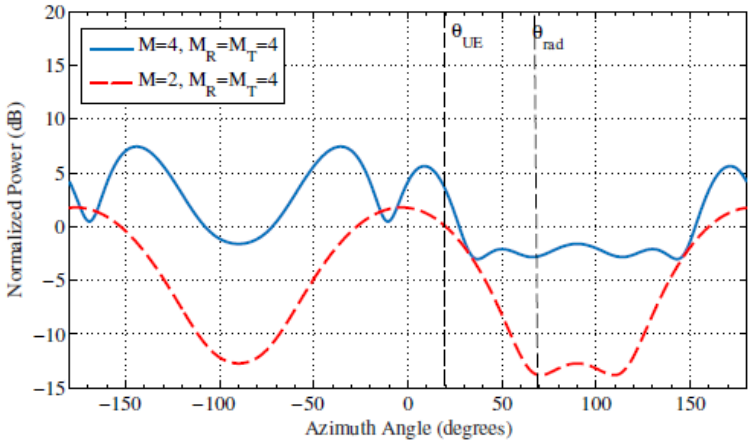

(a)

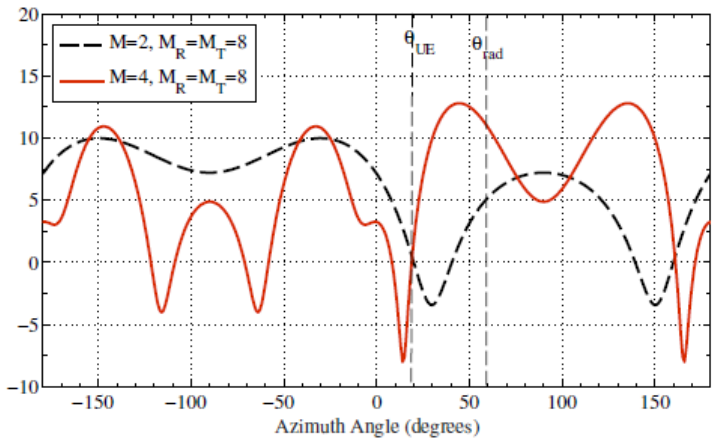

(b)

Fig. 35: BS Array Response with LCMV Beamforming Weights.

5.9 Robust Transceiver Design in Full-Duplex MIMO Cognitive Radios

In this section, we study a full-duplex (FD) multiple-input multiple-output (MIMO) cognitive cellular network, in which a secondary base-station (BS) operating in FD mode serves multiple uplink (UL) and downlink (DL) SUs operating in HD mode simultaneously. The spectrum is shared between secondary and primary networks, and thus uplink SUs and secondary BS generate interference on PUs.

5.9.1 Problem Formulation

We consider a FD multi-user MIMO system that suffers from both self-interference and co channel interference. We assume that the channel state information (CSI) available at the transmitters is imperfect, and the errors of the CSI are assumed to be norm bounded. We take sum-MSE as the performance measure to design the transceivers. Upper limits on both transmit power of the secondary UL users and BS, and interfering power at the PUs are considered. Accordingly, under the impact of channel uncertainty, we address the robust minimization of the sum of mean squared-errors (MSE) of all estimated symbols subject to power constraints at the uplink SUs and secondary BS, and interference constraints projected to each PU. After several mathematical manipulations, we show that this problem can be cast as a Semidefinite programming (SDP), and joint design of transceiver matrices can be obtained through an iterative algorithm. However, the derived optimization problem is not jointly convex over transmit beamforming matrices $\mathbf{V}$ and receiving beamforming matrices $\mathbf{U}$, but is component-wise convex over $\mathbf{V}$ and $\mathbf{U}$, i.e., for fixed $\mathbf{U}$, the problem is convex with respect to $\mathbf{V}$ and vice versa. Therefore, we will employ an iterative algorithm that finds the efficient solutions of $\mathbf{V}$ and $\mathbf{U}$ in an alternating fashion until convergence or a pre-defined number of iterations is reached. The algorithm for the sum-MSE optimization problem that uses SDP method is given in Table I.

TABLE I: Sum-MSE Minimization using SDP Algorithm

---

1) Set the iteration number n = 0 and initialize $\mathbf{V}^{[n]}$.
2) $n \leftarrow n + 1$. Update $\mathbf{U}_i^{[n]}$, $i \in S$ by solving the convex SDP problem under fixed $\mathbf{V}^{[n-1]}$.
3) Update $\mathbf{V}_i^{[n]}$, $i \in S$ by solving the convex SDP problem under fixed $\mathbf{U}^{[n]}$.
4) Repeat steps 2 and 3 until convergence or a predefined number of iterations is reached.

Since the proposed sum-MSE algorithm monotonically decreases the total MSE over each iteration by updating the transceivers in an alternating fashion,and the fact that MSE is bounded below (at least by zero), it is clear that the proposed sum-MSE minimization algorithm is convergent and is guaranteed to converge to a stationary minimum. Since the sum-MSE optimization problem is not jointly convex, the proposed algorithm is not guaranteed to converge to a global optimum point.

5.9.2 Key results

We numerically compare the proposed algorithm with the HD algorithm under the 3GPP LTE specifications for small cell deployments. A single hexagonal cell having a BS in the center with $M_0 = 2$ transmit and $N_0 = 2$ receive antennas with randomly distributed K = 3 UL and J = 3 DL users equipped with 2 antennas is simulated. The cognitive radio system has L = 2 PUs, with the same maximum allowed interfering power. The channel between BS and users (both SUs and PUs) are assumed to experience the path loss model for line-of-sight (LOS), and the channel between UL and DL users are assumed to experience the path loss model for non-line-of-sight (NLOS) communications. The cell radius is considered to be 40m, carrier frequency: 2GHz, bandwidth: 10MHz, thermal noise density: -174dBm/Hz, noise figure for BS: 13dB/ user: 9dB, path loss (dB) between BS and users (d in km): $103.8 + 20.9 \log_{10} d$, path loss (dB) between users (d in km): $145.4 + 37.5 \log_{10} d$ and shadowing standard deviation for LOS: 3dB/ NLOS: 4dB.

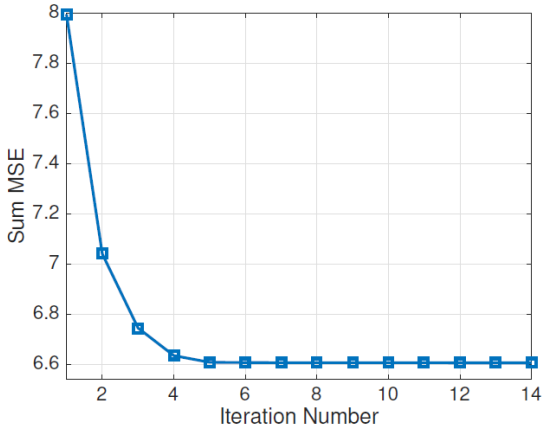

Fig. 36: Convergence of the proposed algorithm

Fig. 36 shows the evolution of the proposed algorithm, i.e., the convergence of the algorithm in Table I. The monotonic decrease of the sum-MSE can be verified, and is seen to converge quite rapidly.

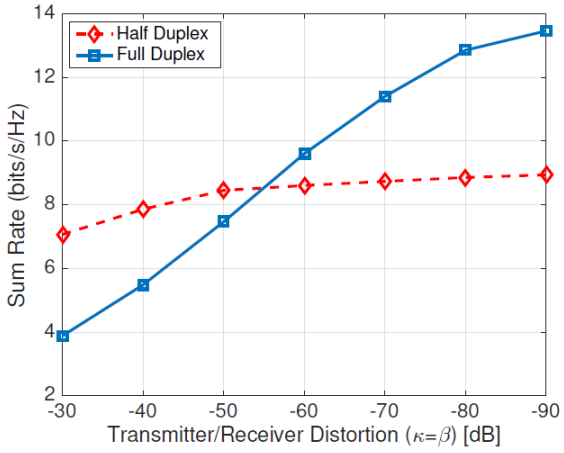

Fig. 37: Sum-rate comparison of FD and HD systems with respect to transmitter/receiver distortion

We then compare FD with HD systems in terms of sum-rate performance. As seen in Fig. 37, the performance of HD system is not affected with κ and β values, and at high self-interference cancellation levels, FD systems achieves around 1.6 times more sum-rate than that of HD, and the performance of FD system drops below that of HD scheme around $\kappa = \beta$ = -55dB.

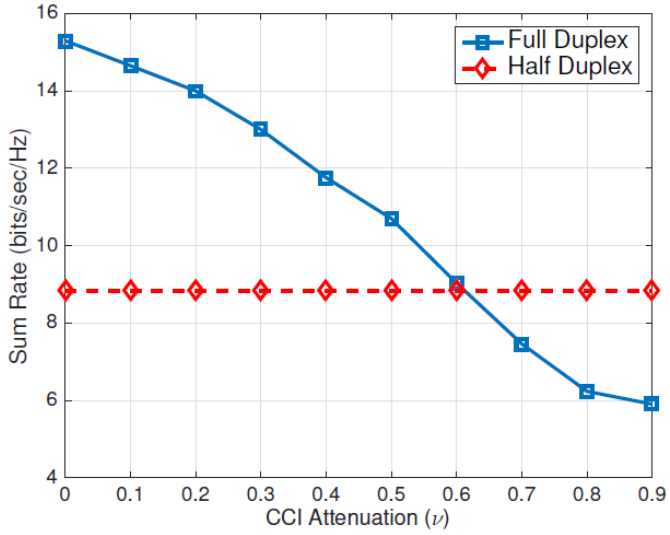

Fig. 38: Sum-rate comparison of FD and HD systems with respect to CCI attenuation factor

It is important to note that while the channel matrices are assumed to be given for each user, it is essential for a practical system to exploit a smart channel assignment algorithm prior to precoder/decoder design. This is particularly essential for a FD setup as the CCI can be reduced by assigning the users with weaker interference paths into the same channel. In order to incorporate the effect of channel assignment into our simulation, we assume an attenuation

coefficient, namely, ν, on the CCI channels, which represent the degree of isolation among UL and DL users due to channel assignment. In Fig. 38, the importance of the smart channel assignment, as a stage prior to the precoder/decoder design is depicted. The CCI attenuation represents the provided isolation among the UL and DL users. As the suppression level of CCI increases, the FD system starts outperforming the HD system, and thus isolation among the UL and DL users is essential for a successful coexistence of UL and DL users in a FD setup.

6. Summary and conclusions

In this deliverable, we have presented a number of optimization problems and their solutions in an algorithmic form, with reference to multiple antenna LSA systems, in the existence of cooperation and coordination. Cooperation can be existent between incumbent and licensee systems, as well as between nodes belonging to a licensee system.

In section 5.1, a new cost-efficient allocation scheme of antennas and spectrum has been proposed for the small-cell/C-RAN scenario. Since the number of distributed antennas in a system is finite and the available spectrum can be expensive in terms of financial cost, an algorithm of distributing the above resources to potential licensees has been developed and numerical simulations show that the cost-efficiency of the network can be significantly increased in comparison to the uncoordinated case, where either the number of antennas or the bandwidth are maximized.

In section 5.2, a novel statistically coordinated LSA precoding scheme has been proposed, in the existence of local CSIT of different quality (i.e., instantaneous or statistical), which can be applicable to the macro-cell scenario. It is supposed that the incumbent and licensee systems are both in transmission mode and both transmitters cooperate in terms of solving the same optimal precoding problem. The search space is reduced to a representative set of joint precoding schemes and the optimal one (in terms of maximizing the average rate of the licensee) is selected, which also importantly satisfies a QoS constraint on incumbent communication. Both transmitters converge to the same solution, and this is guaranteed by the knowledge of channel statistics that is commonly known. Significant throughput gains are reported in comparison to the classical underlay CR approach, thus, a licensee can more easily achieve and sustain its throughput-based targets.

In section 5.3, a hybrid transmission/reception approach has been proposed for the licensee system, by focusing on a macro-cell multiple antenna LSA system, both in the uplink and in the downlink. The hybrid nature of the licensee's operation lies in the SS results, which means that the licensee transmission policy (i.e., power allocation in the downlink, receive BF in the uplink) strongly depends on the SS results. Consequently, optimization problems have been formulated, which focus on the maximization of the average rate of the licensee receiver, subject to an outage-based constraint on incumbent communication. In order to solve these problems, closed form expressions or closed form approximations of the involved quantities have been derived and their validity has been numerically verified. Having obtained such expressions, the problems of a). Optimizing the SS parameters for the downlink communication problem and b). Jointly optimizing

the SS parameters and the receive filter applied at the licensee receiver, for the uplink communication problem, have been solved. The performance potential of the optimized hybrid LSA system has been evaluated by means of simulation and significant gains in spectral efficiency have been observed, compared to schemes taken from the CR literature.

In section 5.4, we studied simple cooperation schemes for dynamic LSA. As the numerical simulation results have illustrated, these schemes boost the performance of the overall system while respecting the predefined QoS constraints. This work emphasized two things: a) the importance of sharing the performance measurements between the incumbent and the licensee; and b) the feasibility and efficiency of low feedback overhead techniques under the LSA framework.

Section 5.5 considered the train scenario in which the high mobility leads to Intercarrier Interference (ICI) in OFDM communication systems. However, even at TGV speeds, it turns out that in a typical LTE setting, the channel time variation over an OFDM symbol duration can be adequately modelled by a linear variation. MIMO transmission techniques are then developed in which the excess multiple antennas over the spatial multiplexing are exploited to adequately suppress the ICI. Future work needs to consider extensions to imperfect CSIT because in the high mobility scenario considered, CSIT acquisition delay will require channel prediction and lead to channel prediction errors.

Section 5.6 studied LSA coordinated beamforming between incumbent and licensee cells. Optimized beamforming techniques are introduced to maximize a joint weighted sum utility function. These techniques are furthermore extended to the case of partial CSIT, with a practical approximation of the ergodic sum utility function, which becomes exact in the Massive MIMO setting. It is shown that this coordinated beamforming approach can be considered as an extension of traditional underlay cognitive radio approaches with interference temperature constraints. The Lagrange multiplier for the interference constraint gets replaced in coordinated beamforming by a value that optimally reflects the joint utility function.

In section 5.7, we developed the full-duplex spectrum sensing system to realize the simultaneous spectrum sensing and secondary transmission. Firstly, the generalized expressions of the key sensing performance metrics are derived for multiple sensing antennas. Listen-and-talk protocol is applied and multiple sensing/transmission antennas are considered in this part. Secondly, the optimal decision threshold pair is investigated in order to minimize the total error rate of the system. Therefore, the benefits of primary and secondary users can be considered at the same time.

In section 5.8, we worked on the problem of effective spectrum sharing between a collocated Multiple-Input-Multiple-Output (MIMO) radar that monitors the existence of a target and a wireless communications system. We presented an accurate model for the operation of the wireless system in the downlink, while the MIMO radar tries to maintain an acceptable detectability level of a target in the far field. The target detection problem was reformulated using a sensing approach based on energy detection, while the BS applies beamforming to null the interference created at the radar receiver. Based on the theory of Hermitian quadratic forms and with the aid of the Linearly Constrained Minimum Variance (LCMV) beamforming solution, the performance of target

detection, when the MIMO radar coexists with the data transmission wass quantified and numerical results show that spectral coexistence is feasible.

In section 5.9, we considered a FD multi-user MIMO system that suffers from both self-interference and co channel interference. The sum-MSE was taken as the performance measure to design the transceivers. Upper limits on both transmit power of the secondary UL users and BS, and interfering power at the PUs were considered. Accordingly, under the impact of channel uncertainty, we addressed the robust minimization of the sum of mean squared-errors (MSE) of all estimated symbols subject to power constraints at the uplink SUs and secondary BS, and interference constraints projected to each PU. After several mathematical manipulations, we showed that this problem can be cast as a semidefinite programming (SDP), and joint design of transceiver matrices can be obtained through an iterative algorithm.